(12)

WT-120(EX)
EXTRACTED VERSION

OPERATION GREENHOUSE

Scientific Director's Report of Atomic Weapon Tests at Eniwetok, 1951
Annex 1.3—Thermal Radiation Measurements
Part I, Atmospheric Transmission
Part II, Total Thermal Radiation
Part III, Radiant Power as a Function of Time--Photoelectric Measurements
Appendix A, Identification of the Teller Light Emission Spectrum
Appendix B, Atlas of High Dispersion Spectra

C. C. Petty
L. F. Drummeter, Jr.
J. A. Curcio
Naval Research Laboratory
Washington, DC

September 1961

NOTICE:

This is an extract of WT-120, Operation GREENHOUSE, Annex 1.3, Parts I, II, and III, and Appendices A and B.

Extracted version prepared for
Director
DEFENSE NUCLEAR AGENCY
Washington, DC 20305-1000

1 September 1985

Destroy this report when it is no longer needed. Do not return to sender.

PLEASE NOTIFY THE DEFENSE NUCLEAR AGENCY, ATTN: STTI, WASHINGTON, DC 20305-1000, IF YOUR ADDRESS IS INCORRECT, IF YOU WISH IT DELETED FROM THE DISTRIBUTION LIST, OR IF THE ADDRESSEE IS NO LONGER EMPLOYED BY YOUR ORGANIZATION.

DNA PRINTING PLANT

UNCLASSIFIED
SECURITY CLASSIFICATION OF THIS PAGE

AD-A995 353

REPORT DOCUMENTATION PAGE

1a REPORT SECURITY CLASSIFICATION UNCLASSIFIED	1b RESTRICTIVE MARKINGS
2a SECURITY CLASSIFICATION AUTHORITY N/A since Unclassified	3 DISTRIBUTION / AVAILABILITY OF REPORT Approved for public release; distribution is unlimited.
2b DECLASSIFICATION / DOWNGRADING SCHEDULE N/A since Unclassified	
4 PERFORMING ORGANIZATION REPORT NUMBER(S)	5 MONITORING ORGANIZATION REPORT NUMBER(S) WT-120 (EX)
6a NAME OF PERFORMING ORGANIZATION Naval Research Laboratory 6b OFFICE SYMBOL (If applicable)	7a NAME OF MONITORING ORGANIZATION Defense Atomic Support Agency
6c ADDRESS (City, State, and ZIP Code) Washington, DC	7b. ADDRESS (City, State, and ZIP Code) Washington, DC
8a. NAME OF FUNDING / SPONSORING ORGANIZATION 8b. OFFICE SYMBOL (If applicable)	9 PROCUREMENT INSTRUMENT IDENTIFICATION NUMBER
8c. ADDRESS (City, State, and ZIP Code)	10 SOURCE OF FUNDING NUMBERS PROGRAM ELEMENT NO. / PROJECT NO / TASK NO. / WORK UNIT ACCESSION NO.

11 TITLE (Include Security Classification) OPERATION GREENHOUSE, Scientific Director's Report of Atomic Weapon Tests at Eniwetok, 1951; Annex 1.3—Thermal Radiation Measurements; Parts I, II, and III; Appendices A and B, Extracted Version

12 PERSONAL AUTHOR(S)
Petty, C.C.; Drummeter, L.F., Jr.; and Curcio, J.A.

13a TYPE OF REPORT	13b TIME COVERED FROM ____ TO ____	14 DATE OF REPORT (Year, Month, Day)	15 PAGE COUNT
		6109	80

16 SUPPLEMENTARY NOTATION This report has had sensitive military information removed in order to provide an unclassified version for unlimited distribution. The work was performed by the Defense Nuclear Agency in support of the DoD Nuclear Test Personnel Review Program.

17 COSATI CODES		
FIELD	GROUP	SUB-GROUP
18	3	
20	13	

18. SUBJECT TERMS (Continue on reverse if necessary and identify by block number)
Greenhouse; Atmospheric Transmission; Thermal Radiation; Teller Light; Radiation Measurements

19 ABSTRACT (Continue on reverse if necessary and identify by block number)

Atmospheric transmission measurements were most important to the thermal program since they gave the information which was necessary to compute and cancel out the effects of intervening air paths on measurements of total thermal energy, radiant energy, radiant power with respect to time, and spectral emission of the bombs.

The brightness temperature of each of the Operation Greenhouse fireballs was measured in two wavelength regions as a function of time. The measurements were made with high-speed filtered photoelectric systems located at Parry Island.

The Teller Light phenomena is also covered. The Thermal Radiation Project included specific objectives of recording the spectra of the release of visible and ultraviolet radiation by an exploding nuclear weapon in three stages: Teller Light, first maximum, and second maximum.

20 DISTRIBUTION / AVAILABILITY OF ABSTRACT ☒ UNCLASSIFIED/UNLIMITED ☐ SAME AS RPT ☐ DTIC USERS	21 ABSTRACT SECURITY CLASSIFICATION UNCLASSIFIED
22a NAME OF RESPONSIBLE INDIVIDUAL MARK D. FLOHR	22b TELEPHONE (Include Area Code) (202) 325-7559 22c. OFFICE SYMBOL DNA/ISCM

DD FORM 1473, 84 MAR 83 APR edition may be used until exhausted
All other editions are obsolete.

SECURITY CLASSIFICATION OF THIS PAGE
UNCLASSIFIED

FOREWORD

Classified material has been removed in order to make the information available on an unclassified, open publication basis, to any interested parties. The effort to declassify this report has been accomplished specifically to support the Department of Defense Nuclear Test Personnel Review (NTPR) Program. The objective is to facilitate studies of the low levels of radiation received by some individuals during the atmospheric nuclear test program by making as much information as possible available to all interested parties.

The material which has been deleted is either currently classified as Restricted Data or Formerly Restricted Data under the provisions of the Atomic Energy Act of 1954 (as amended), or is National Security Information, or has been determined to be critical military information which could reveal system or equipment vulnerabilities and is, therefore, not appropriate for open publication.

The Defense Nuclear Agency (DNA) believes that though all classified material has been deleted, the report accurately portrays the contents of the original. DNA also believes that the deleted material is of little or no significance to studies into the amounts, or types, of radiation received by any individuals during the atmospheric nuclear test program.

Scientific Director's Report of Atomic Weapon Tests at Eniwetok, 1951

Annex 1.3

THERMAL RADIATION MEASUREMENTS

CONTENTS

Part I Atmospheric Transmission

Part II Total Thermal Radiation

Part III Radiant Power as a Function of Time —Photoelectric Measurements

ILLUSTRATIONS

Part I Atmospheric Transmission

Part II Total Thermal Radiation

Part III Radiant Power as a Function of Time

ILLUSTRATIONS (Continued)

Appendix A Identification of the Teller Light Emission Spectrum

TABLES

Part I Atmospheric Transmission

Part II Total Thermal Radiation

Part III Radiant Power as a Function of Time — Photoelectric Measurements

TABLES (Continued)

Appendix A Identification of the Teller-Light Emission Spectrum

Part I
Atmospheric Transmission

Radiometry Branch, Optics Division
Naval Research Laboratory
Washington, D. C.

August 1958

ABSTRACT

Several techniques were used to measure the transmission of the atmosphere at Operation Greenhouse. Spectral transmission measurements were made over a horizontal path between Parry and Eniwetok Islands at H – 1 hr for each shot. A recording photoelectric transmissometer was operated over a slant path from shot-tower cab to ground station for the Dog and Easy shots.

The attenuation coefficient obtained over the slant path was lower than that obtained over the horizontal path for the same wavelength. The higher attenuation over the horizontal path was assumed to be caused by nonselective scattering from large particles close to the water surface. This effect is constant for each wavelength; thus each horizontal-path coefficient was adjusted by the same amount to give appropriate slant-path spectral attenuation coefficients. This method was used for the Dog and Easy shots.

No slant-path transmissometer data were available on the George and Item shots; therefore it was necessary to arrive at the slant-path transmission in an indirect manner. It is shown that a knowledge of the ratio between the thermal fluxes received at any two distances leads directly to a measure of the atmospheric transmission. A comparison of this data with the transmissometer data from Dog shot demonstrates that this indirect method leads to correct results.

In support of measurements of total thermal radiation, it was necessary to determine the transmission of the atmosphere in the near-infrared region of 0.7 to 12 μ for each of the shots. Since measurements were not made, this information had to be derived from the spectral transmission data for the visible region, utilizing knowledge of fireball-color temperature, atmospheric conditions, and published information on absorption in the infrared. The final composite transmission figures used for the evaluation of total thermal data are presented.

PREFACE

This report describes the atmospheric transmission investigations carried out at Operation Greenhouse by the Radiometry Branch of the Optics Division, U. S. Naval Research Laboratory (NRL). The work was carried out under the direction of Harold S. Stewart and was part of the over-all program of measurements carried out under the general supervision of Wayne C. Hall.

The techniques for the measurement of spectral transmission were developed at NRL and were tested at the Chesapeake Bay Annex of NRL by Joseph A. Curcio, C. Preston Butler, Charles C. Petty, Louis F. Drummeter, and H. S. Stewart.[1] Methods for field measurement were tested at Dry Tortugas, Florida, by the above group, assisted by Donald J. Lovell, Carl A. Pearson, and Burt S. Engel.

Atmospheric transmission as a function of wavelength was measured at Operation Greenhouse by C. C. Petty, J. A. Curcio, and Alcide Santilli, Captain, USA (Signal Corps).

Measurements of the slant-path atmospheric transmission between the cab of the shot tower and certain of the NRL stations were recorded using equipment developed by C. A. Pearson and operated at Operation Greenhouse by L. F. Drummeter.

This report was prepared by Edward M. Man. The assistance of Dorothy E. Buttrey and the Graphic Arts Section of NRL is acknowledged.

1 OBJECTIVE

Measurements of atmospheric transmission as a function of wavelength served a twofold purpose at Operation Greenhouse. The measurements were most important to the thermal program since they gave the information which was necessary to compute and cancel out the effects of intervening air paths on measurements of total thermal energy, radiant power with respect to time, and spectral emission of the bombs. Another function of the measurements was operational in that they were used to indicate whether it was raining between the zero point and the instrument station. For the Easy shot this was the primary transmission responsibility because of the extensive effects program.

2 BACKGROUND

2.1 General Remarks

It is known that for wavelengths between 0.32 and 0.7 μ, atmospheric attenuation is primarily due to scattering of three types: (1) molecular scattering, described by Rayleigh;[3] (2) scattering by small particles, selective with wavelength and described by Stratton and Houghton;[4] and (3) scattering by large particles, essentially nonselective with wavelength. For wavelengths shorter than 0.32 μ, true absorption by ozone and oxygen occurs in the atmosphere in addition to molecular scattering.[5] For wavelengths greater than 0.7 μ, two attenuation processes of major importance are (1) the selective absorption by water vapor and carbon dioxide in the air[6,7] and (2) the scattering by haze and dust particles suspended in the air.[7]

The spectral transmission of the atmosphere in the ultraviolet and the visible portions of the spectrum cannot be uniquely determined through measurement of the atmospheric transmission at one wavelength because the concentration of ozone appears to vary from day to day, as does the ratio of large-to-small particle scattering.[5] In the near-infrared portion of the spectrum the determination is even more difficult. On one hand very little information is available as to scattering, which is a function of haze concentration. On the other hand measurements of the absorption concentrated in discrete water vapor and carbon dioxide bands are difficult.

Values quoted for the transmission of the atmosphere are usually related to that fraction of incident flux which will penetrate a given path length without deviation by scattering. Lambert's law of attenuation is

$$T(\lambda,D) = e^{-\alpha_\lambda D} \tag{1}$$

where $T(\lambda,D)$ is the transmission for the wavelength λ over a path length of D kilometers, e is the natural logarithm base, and α_λ, having the dimensions of inverse distance, is the atmospheric attenuation coefficient for the wavelength λ.

2.2 Development of Techniques

The techniques used at Operation Greenhouse for the measurement of spectral transmission of the atmosphere were developed at the U. S. Naval Research Laboratory (NRL) and tested at the Chesapeake Bay Annex (CBA) of NRL and at Dry Tortugas, off the coast of Florida. Methods have been described in detail in the NRL-H Greenhouse Preoperational Report[8] and also in the Journal of the Optical Society of America.[1]

At CBA and Dry Tortugas, transmission measurements were made at night over horizontal paths roughly five miles in length, using the emission lines in the wavelength interval 2500 to 6000 A from a mercury-arc source. For all observations made the values of the spectral atmospheric attenuation coefficients (km^{-1}) were computed. These values increase toward the shorter wavelengths and this effect is most pronounced for wavelengths below 3200 A, where true absorption as well as scattering contributes to the attenuation.

The technique used for the measurement of slant transmission was developed at NRL by C. A. Pearson.[2,3] The equipment was designed to record transmission at night in weather for which the total transmission of the atmosphere in the visible region of the spectrum varied from 20 to 85 per cent over a 4-km path. The measurement of the transmission of visible light by such a photoelectric method required a phototube and filter combination with a maximum spectral response to the light source in agreement with that of the eye.

2.3 Procedure for Dog and Easy Shots Data Reduction

2.3.1 Slant-path Transmission

The light path used for spectral transmission measurements at Operation Greenhouse was about 6 ft above a reef, and, without question, spray particles affected the results so that the attenuation coefficients could not be taken as representative of the slant transmission path between the cab on a shot tower and any observing station. It proved impractical to measure spectral attenuation coefficients over the slant paths actually employed in the several shots; therefore a supplementary method was used which enabled the application of horizontal attenuation coefficients to the slant paths.

The photoelectric transmissometer was operated for the Dog and Easy shots several feet above sea level, the light source being mounted on the cab of the shot tower at a slant-path distance of approximately 5 km from the transmissometer. The spectral distribution of the source radiation and the spectral response of the phototube-filter combination were such that the transmission measured by the transmissometer corresponded to the transmission for a fairly narrow wavelength band centered at 5500 A.

As was expected, the slant attenuation coefficient indicated by the transmissometer was lower than the value for the horizontal attenuation coefficient obtained for 5461 A from the spectrographic plates taken at the same time. The difference between the above values (horizontal α_λ and slant α_λ), β_λ, was assumed to be the attenuation over the horizontal path caused by nonselective scattering from large particles close to the water. In general, large-particle scattering is constant for each wavelength; hence $\beta_\lambda = \beta$. Slant-path spectral attenuation coefficients were obtained by subtracting β from each of the measured horizontal coefficients for the various mercury lines. These calculated values represent the slant-path spectral attenuation coefficients which were applied to all measurements made from ground observing stations.

2.3.2 Transmission in the Near-infrared

In support of measurements of total thermal radiation, it was necessary to determine the effective transmission of the atmosphere in the near-infrared region of 0.7 to 12 μ for each of the shots at Operation Greenhouse. Since measurements were not made directly, this information had to be derived from the slant-path spectral transmission data for the visible region utilizing knowledge of fireball-color-temperature, atmospheric conditions, and published information on absorption in the infrared (references 4, 5, and 9 to 11).

The following data should be considered in order to better understand the nature of the transmission factor necessary for correction of the total thermal radiation data.

Assume that the flux radiated by the source is separated into two spectral regions of wavelengths shorter than and longer than 0.7 μ. Thus, without considering the intervening atmosphere, the total flux can be represented by

$$F = F_v \text{ (below } 0.7\mu) + F_i \text{ (above } 0.7\mu) \tag{2}$$

The choice of 0.7 μ can be considered to distinguish between the visible and infrared portions of the spectrum.

For an attenuating atmosphere the observed flux F′ could be given by

$$F' = T_v F_v + T_i F_i \tag{3}$$

where T_v would be an average transmission factor appropriate for a given distribution of flux in the visible region and T_i a factor appropriate for the distribution in the infrared. Also F′ would be related to the vacuum flux F by

$$F' = TF \tag{4}$$

where the composite transmission factor, T, is given by

$$T = T_v(F_v/F) + T_i(F_i/F) \tag{5}$$

The ratios F_v/F and F_i/F are the fractions of the total flux below and above 0.7 μ. By knowing the fireball-color temperature and assuming a black-body energy distribution, these fractions can be determined. T_v was measured. This leaves T_i to be determined in order to calculate T–the factor needed to translate F′ into F.

The infrared transmission factor, T_i, in itself is a composite factor giving the attenuation due to both scattering and absorption. The assumption is made that T_i (scattering and absorption) = T_i (scattering) × T_i (absorption). To simplify the calculations, T_i (scattering) is assumed equal to T_v. Thus it is left to find T_i (absorption). This quantity is determined by the process outlined in reference 9.

It must be kept in mind that a further complication to this problem is that all of the above-mentioned transmission factors must be corrected for aureole (see Sec. 2.5).

2.3.3 Effective Transmission

As indicated in the previous section, for correction of the total thermal radiation data, composite transmission factors must be determined. To a first approximation, the flux below 0.7 μ is treated differently and independently of the flux above 0.7 μ. Because of the fields of view involved, each thermal instrument at each shot had a unique transmission factor which we will refer to as the effective transmission for instrument A at shot B. All such factors are given in Table 7.

2.4 Procedure for George and Item Shots Data Reduction

2.4.1 Indirect Determination of Slant-path Transmission

In the case of the George and Item shots, although the spectral transmission coefficients were measured for the horizontal paths as before, no slant-path transmissometer data were available for the direct slant-path normalization. Therefore it was necessary to determine slant-path transmission in an indirect manner.

The method used was based on the assumption that the ratio between the value of total thermal energy received at each of two stations leads to a measure of the slant-path transmission. This was justified theoretically, but some question remained as to the feasibility of this method in terms of the reliability of results obtained by the actual computation. A check was

made by computing the slant-path attenuation coefficient by this method for Dog shot, for which transmissometer data were available. The agreement between computed and measured values was good; hence the indirect method of determination was deemed sufficiently accurate to give reliable figures for slant-path transmission. The theoretical justification and the assumptions made are given in Appendix 1, this part.

2.4.2 Effective Transmission

After the slant-path transmission had been determined by the indirect method outlined in Sec. 2.4.1, composite transmission factors for correction of the total thermal data could be found as indicated in Sec. 2.3.3. These factors are also given in Table 7.

2.5 Field of View

When transmission of the atmosphere is determined by comparing the measured illuminance due to a distant light source to the calculated value given by the inverse square law, the result obtained is dependent upon the field of view of the receiver. This field-of-view dependency is due to aureole, which is the result of light being scattered into the field of view by constituents of the air. This scattered flux augments that coming directly from the source. However it has been shown that for the short paths and the small fields of view used in the transmissometers and spectrographs this correction is negligible.[12] On the other hand the instruments used to obtain thermal data possessed large fields of view and, therefore, the transmission data given in this report must be adjusted before applying them to the thermal measurements.

2.6 Mirage and Refractive Effects

The Dry Tortugas work had indicated that mirage effects can distort horizontal transmission measurements.[1] The effect of any mirage in the data taken at Operation Greenhouse was negligible for slant observations.

In addition, careful observations made just prior to each shot, in order to determine the possible existence of refraction along the horizontal path, showed no such effects. It is unlikely that the spectral data recorded at Parry Island will suffer from this type of error.

3 INSTRUMENTATION

3.1 Spectral Transmission Measurements

Light from a mercury arc located on the southern tip of Parry Island was concentrated on the slit of a low-dispersion quartz-prism spectrograph by means of a concave mirror of short focal length. The distance from the light source to the spectrograph was 5 m. A second spectrograph and a longer focal-length mirror were located on Eniwetok Island at a distance of 6.56 km from the source of light. Simultaneous exposures were made on the two spectrographs by shuttering the light source. The choice and arrangement of mirrors was such that the slit of each spectrograph would have the same illuminance in the absence of attenuation by the atmosphere. Therefore the observed ratio of photographic exposure of the spectral lines in the two spectrograms permitted computation of the atmospheric attenuation coefficient at each measured wavelength.[1]

The field of view of each spectrograph was limited to one-half degree to eliminate the effect of aureole due to forward-scattered light,[12] and exposure times of 30 sec were used to average out intensity fluctuations due to twinkle.

A schematic diagram of the experimental arrangement used is shown in Fig. 1. The

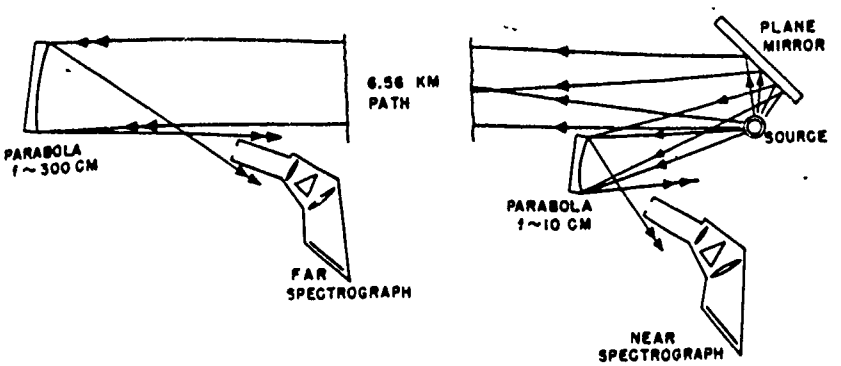

Fig. 1—Schematic drawing of optical arrangement for spectral transmission measurements.

mercury-arc source was a 5500-watt quartz-jacketed lamp made by the Hanovia Lamp Division of Engelhard Industries, Inc. The quartz tube had a useful length of 55 in. and was about 1 in. in diameter. It was mounted in front of a plane mirror with its long axis vertical so that from the direction of the spectrographs there appeared to be two lamps side by side, thus increasing the effective flux by approximately a factor of 2. The front-surfaced plane mirror was made of several sections of selected plate glass on which aluminum had been evaporated. The concave mirrors had simultaneously evaporated aluminum surfaces, hence very nearly the same reflection properties.

The spectrographs were two identical Hilger E-31 quartz-prism instruments. Wide slits were used on the spectrographs to simplify the densitometry of the images. No slit-width correction is necessary with a mercury-arc line source, hence the slit-width settings could be made without particular care. An evaporated platinum-step wedge was mounted directly in front of the slit of each spectrograph. Eastman type No. I-F or III-F spectrographic plates were used; for each transmission run the two plates were processed simultaneously by brush development in Eastman D-19 developer.

3.2 Recording D-C Transmissometer

The d-c transmissometer used for measurements of slant-path transmission is described in detail in references 3 and 4.

A vertical cross-section diagram of the optical components of the photoelectric transmissometer is shown in Fig. 2. Lens L_2 was placed so as to produce an image of lens L_1 on

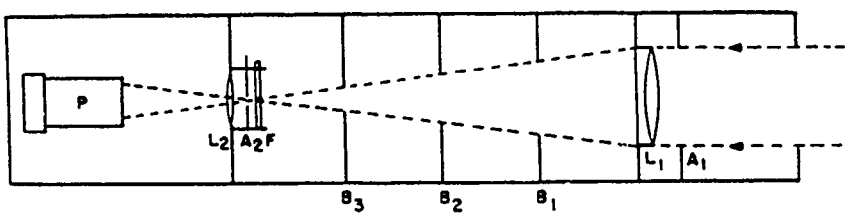

(A_1) VARIABLE APERTURE ($L_1 L_2$) LENSES
(A_2) FIXED APERTURE (F) FILTER
($B_1 B_2 B_3$) BAFFLES (P) MULTIPLIER PHOTOTUBE

Fig. 2—Optical diagram of photoelectric transmissometer.

the sensitive surface of photomultiplier P. The multiplier phototube selected was an RCA 5819. Its spectral response to a 2850°K tungsten source was in close agreement with that of the human eye and its photosensitive surface was large and conveniently placed. The output from the

phototube was fed into a direct-current amplifier which consisted of a cathode follower, to match the high impedance of the phototube to the low impedance of the Esterline-Angus recorder, and a zero balance section, so that the recorder could be set to read zero for zero input. The transmissometer-recorder installation is shown in Fig. 3. The chart record shown is indicative of the type of information obtained. The sudden cutoff in signal represents the time of explosion.

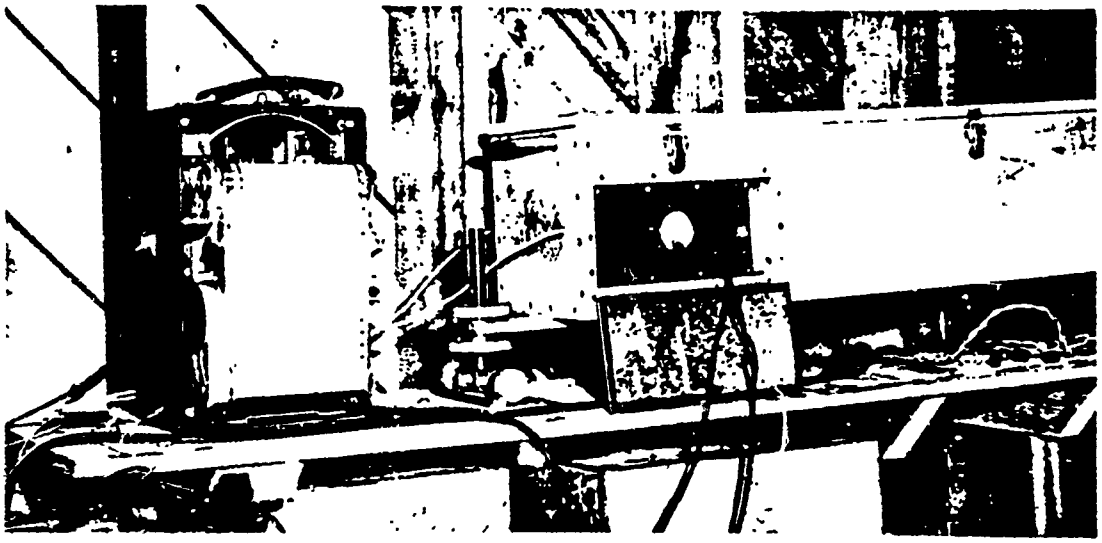

Fig. 3—Photoelectric-transmissometer installation showing typical shot-time data.

The distant light source of the transmissometer was a bare 1000-watt projection type lamp. This type of lamp had suitable candle power (about 1400 cp at 2850°K) for a range of 4 km and for the sensitivity of the transmissometer.

Absolute calibration of the transmissometer was made with a small standard lamp (such as used in the Macbeth illuminometer) at a temperature of 2360°K. (In the field a Wratten 86B filter of known transmission was placed in front of the telephotometer to reduce the color temperature of the 1000-watt lamp to 2360°K. This resulted in a higher intensity than would have been obtained if the sources themselves had been operated at a color temperature of 2360°K.) The relationship between illuminance at the receiver and readings at the recorder was linear.

3.3 Modified Transmissometer

In addition to the standard transmissometer, a modified transmissometer for use over a 30-km path was used at Easy shot. The modifications made on the standard transmissometer to convert its use to the 30-km path are shown in Fig. 4. Lens L_1 was removed and the image of the source was formed at A_2 by a concave mirror with a focal length of 10 ft and a diameter of 16 in.

Calibration of this instrument was made using data from the standard transmissometer. Transmission readings were taken at site P for the slant path to the 300-ft tower on Engebi, and these values were relayed by telephone to Parry Island, where the modified transmissometer was set up to look at the same source on the cab tower at Engebi. The transmission appropriate to the 30-km path was calculated and the modified transmissometer was set to read this calculated value. It was found that the modified transmissometer followed the standard fairly close on subsequent measurements. Along with the standard transmissometer, the

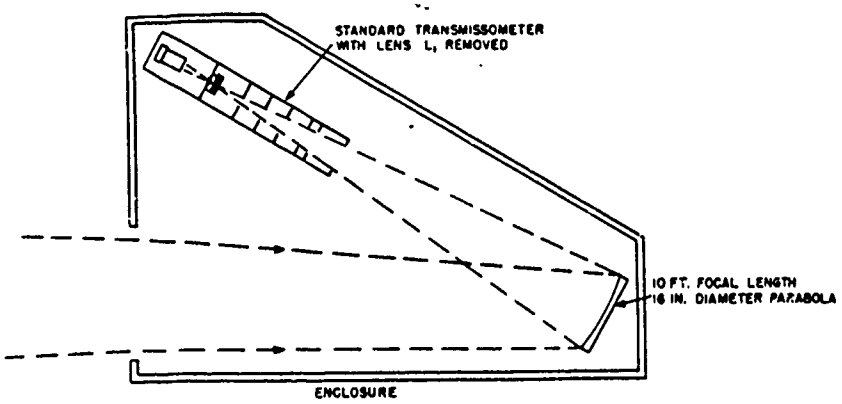

Fig. 4—Optical diagram of standard transmissometer modified for 20-mile path.

modified transmissometer was used in this shot primarily to judge whether it was raining and whether this rain occurred in the 3-km path monitored by the standard instrument or within the 30-km path monitored by the modified version.

3.4 Radiant Flux Measurements

Radiant flux was measured by means of radiation thermopiles which were uniformly black for all wavelengths of thermal radiation (constant absorbtivity). The outputs of the thermopiles were recorded ballistically with photoelectric-recording galvanometers. For each shot, measurements were made at two distances.

A full report on these measurements is given in Part II, Total Thermal Radiation.

3.5 Operational Use of the Instruments

On all shots at Operation Greenhouse, spectral transmission measurements were made over a 6.56-km horizontal path between Eniwetok and Parry Islands every ½ hr for 4 or 5 hr preceding each of the four shots, the last measurements being made at H – 1 hr.

For Dog shot the slant transmissometer was operated at site M, 10 ft above the lagoon, with the light source mounted in the cab of the 300-ft shot tower at a slant-path distance of 3.66 km from the transmissometer. At Easy shot the standard transmissometer was operated at site P, a distance of 5.1 km from the source, mounted in the cab of the shot tower. In addition, as already noted, the modified slant transmissometer was used for this shot operating between shot tower and Parry Island. The information from the standard transmissometer at site P had to be relayed automatically to Parry Island by means of a telemetering cable. Disturbances were such as to cause a change of calibration of the meter to a point that it was only possible to tell if it were raining between site P and the tower. Thus the values of transmission measured along the long path with the modified transmissometer were used in the reduction of thermal data from Easy shot. The location of shot towers, instrument stations, and the paths monitored are shown in Fig. 5.

On the George and Item shots, no slant-path transmissometer data were available for direct slant-path normalization. The slant-path transmission was determined in an indirect way as noted in Sec. 2.4 and Appendix 1, this part. Thermal radiation measurements were made at two different distances from the bomb for each shot; namely, site N and Parry Island for the George shot and site P and Parry Island for the Item shot. These stations and the paths they monitored are also shown in Fig. 5.

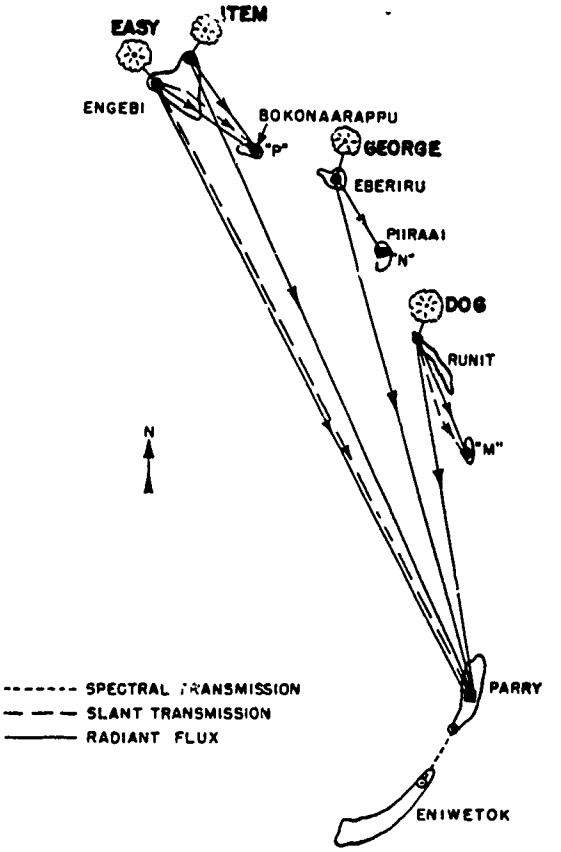

Fig. 5—Station setup for transmission measurements showing paths monitored.

4 RESULTS AND ANALYSIS OF DATA

4.1 Spectral Transmission Measurements

After exposure the plates from each Hilger spectrograph were processed simultaneously. The density of each step at each wavelength for both plates was measured with a Jarrell-Ash microphotometer (see Appendix 2, this part), and a plate characteristic or H and D curve was drawn for each mercury line. The curves for each wavelength from both spectrographic plates were plotted on the same graph. Figure 6 shows a typical plot for wavelength 3660 A, the horizontal separation of the two H and D curves being a measure of the transmission of the atmosphere. Figure 7 shows the spectral attenuation coefficients derived from the H and D curves plotted as a function of wavelength. Table 1 lists the coefficients for the horizontal path taken from a smooth curve through the experimental points in Fig. 7. For each wavelength the numbers represent the value of α in the expression

$$T(\lambda,D) = e^{-(\text{horizontal } \alpha)\, D} \tag{6}$$

where $T(\lambda,D)$ is the specular transmission for the wavelength λ over a path of D kilometers.

4.2 Transmissometer Measurements

A comparison of the illuminances as measured by the transmissometer with that expected for the same path length in a vacuum gave the transmission for that path. From this the trans-

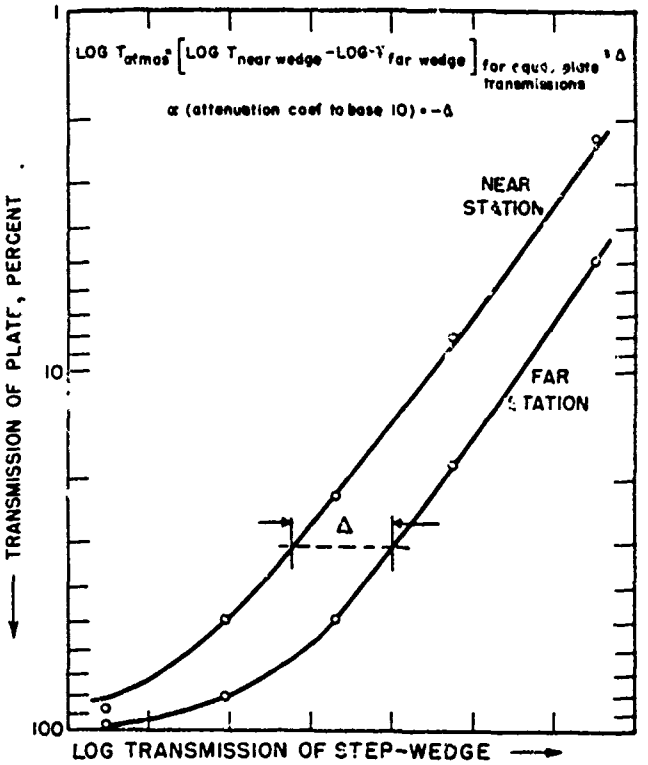

Fig. 6—Typical H and D plot for determination of atmospheric transmission.

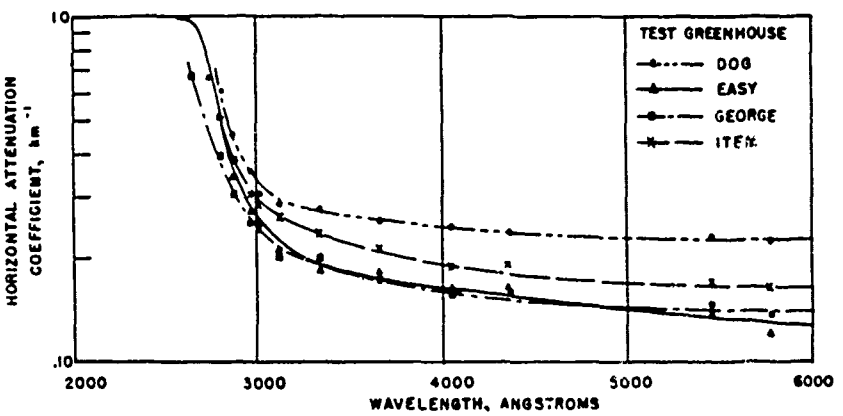

Fig. 7—Horizontal attenuation coefficients vs. wavelength.

mission per kilometer and the slant-path attenuation coefficient were readily determined.

Figure 8 is a typical sample of the transmissometer data as recorded on the Esterline-Angus recorder for the Dog shot. The slant-path attenuation coefficients for the Dog and Easy shots are given in Table 2 along with the pertinent information necessary for the determination of the coefficients. No transmissometer information is available for the George and Item shots.

Table 2 lists both the short- and the long-path values of the coefficient for Easy shot. The short-path data lead to improbable results. This was due to interference from the telemetering line (see Sec. 3.5); hence the long-path value (0.07_4) has been taken as the representative number for atmospheric transmission for the Easy shot.

TABLE 1—SPECTRAL ATTENUATION COEFFICIENTS FOR THE HORIZONTAL PATH

Wavelength, A	Attenuation coefficient, km^{-1}			
	Dog	Easy	George	Item
5780	0.22_5	0.13_0	0.14_1	0.16_5
5460	0.22_6	0.13_4	0.14_5	0.16_7
4360	0.23_6	0.15_5	0.15_2	0.18_0
4050	0.24_2	0.16_4	0.16_0	0.19_0
3660	0.25_6	0.17_5	0.17_2	0.20_0
3340	0.27_0	0.19_2	0.19_0	0.23_5
3130	0.29_5	0.22_3	0.21_7	0.26_2
3020	0.32_8	0.25_5	0.24_1	0.29_2
2970	0.35_5	0.28_0	0.25_8	0.31_4
2890	0.44_5	0.34_8	0.30_8	0.37_6
2805	0.6_0	0.5_2	0.3_8	0.5_2
2750		0.7_1	0.4_5	
2650		0.9_1	0.7_0	

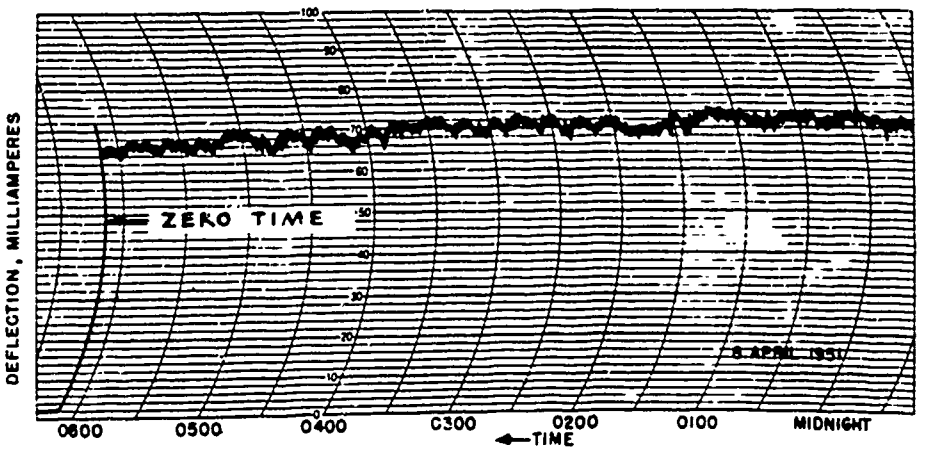

Fig. 8—Slant-path transmission record for Dog shot.

TABLE 2—DETERMINATION OF SLANT-PATH ATTENUATION COEFFICIENTS FROM TRANSMISSOMETER DATA

		Easy	
	Dog	Short path	Long path
Source, cp	1350	2710	2710
Receiver distance, km	3.66	5.1	32.6
Illuminance at receiver (100% transmission), 10^{-4} meter-candles	101	104	25.6
Measured transmission, 10^{-4} meter-candles	67	85	2.3
T_{path}, %	66.7	82	9
T_{km}, %	89.5	96	93
α, km^{-1}	0.11_1	0.03_9	0.07_4

4.3 Transmission as Determined from Thermal Measurements

As indicated in Sec. 4.2, no transmissometer data were available for the George and Item shots. An indirect method involving the total thermal data was evolved as discussed in Sec. 2.4 and Appendix 1, this part.

The equation derived in Appendix 1 enables one to determine the correction factor β (the difference between the slant and horizontal attenuation coefficients) and thus the slant-path transmission from the horizontal transmission and total thermal data. The equation is

$$\beta = \frac{\ln\left[\frac{F_P/F_N\,(D_F/D_N)^2}{\rho}\right]}{D_P - D_N} \tag{7}$$

where

$$\rho = \frac{\int_0^\infty J_\lambda e^{-(\text{horizontal } \alpha_\lambda)D_P}\, d\lambda}{\int_0^\infty J_\lambda e^{-(\text{horizontal } \alpha_\lambda)D_N}\, d\lambda} \tag{8}$$

The quantities represented in Eqs. 7 and 8 are

F_P, F_N = direct flux received at stations P and N, respectively
D_P, D_N = distance from bomb to stations P and N, respectively
J_λ = energy emitted by source per wavelength interval
horizontal α_λ = horizontal attenuation coefficient

An aureole correction must be applied in order to use measured values of flux in Eq. 7. However, this implies a knowledge of atmospheric transmission as well as field of view. Hence β must be determined by a method of successive approximations which involves an aureole correction on the measured flux utilizing, initially, the values of horizontal transmission to stations P and N. This provides "starting" values of the direct fluxes F_P and F_N from which the first approximation value of β can be calculated. This value of β is then fed back into the equation and a second value of β calculated. This process is repeated until the value of calculated β experiences no further change.

The determination of ρ by means of Eq. 8 requires some explanation. The expression is similar to that to be encountered in Sec. 4.5 where transmission in the infrared is discussed. Since the treatment of this type of expression is more pertinent to the discussion of the infrared, only general remarks will be made here.

The integrals of Eq. 8 were actually evaluated over just the visible and near-infrared wavelength regions—separately, as discussed in Sec. 2.3.2. Furthermore, utilizing knowledge of black-body energy distribution and assuming certain things about the transmission in each region, a value for the ratio of fluxes was determined without knowing the actual energy emitted by the source.

The values used for, and to determine, the various quantities in Eqs. 7 and 8 are among the data given in Tables 6 and 7. The correction factors thus determined were for George, $\beta = 0$, and for Item, $\beta = 0$. The correction factor was determined for Dog shot as a check on the method. Comparison of values of β for Dog shot show that, as given by the transmissometer, $\beta = 0.115$ and, as derived from the thermal data, $\beta = 0.104$. The 10 per cent difference is judged acceptable for this work.

4.4 Spectral Attenuation Coefficients for the Slant Path

The spectral attenuation coefficients for the slant path were obtained by subtracting the factor β from each of the values of the horizontal attenuation coefficients given in Table 1.

Table 3 gives the values of β used to determine α_{slant}. Table 4 is the list of spectral attenuation coefficients calculated for the slant path. Figure 9 shows these slant-path coefficients plotted against wavelength.

TABLE 3—VALUES OF THE CORRECTION FACTOR β FOR OBTAINING SLANT-PATH ATTENUATION COEFFICIENTS

Shot	Method of determination	$\alpha_{horizontal}$ (5460 A)	α_{slant} (5500 A)	β
Dog	Standard transmissometer	0.22_6	0.11_1	0.11_5
Easy	Modified transmissometer	0.13_4	0.07_4	0.06_9
George	Thermal data	0.14_2		
Item	Thermal data	0.16_7		

TABLE 4—SPECTRAL ATTENUATION COEFFICIENTS CALCULATED FOR SLANT PATH

Wavelength, A	Attenuation coefficient, km^{-1}			
	Dog	Easy	George	Item
5780	0.11_0	0.07_0	0.12_3	0.12_9
5400	0.11_1	0.07_4	0.11_4	0.13_1
4300	0.12_1	0.09_5	0.12_4	0.14_4
4050	0.12_7	0.10_4	0.13_2	0.15_4
3660	0.14_1	0.11_5	0.14_4	0.17_3
3340	0.15_5	0.13_2	0.16_2	0.19_0
3130	0.18_0	0.16_3	0.18_9	0.22_6
3020	0.21_3	0.19_5	0.21_3	0.25_6
2970	0.24_0	0.22_0	0.23_9	0.27_8
2890	0.33_0	0.28_8	0.28_9	0.34_0
2805	0.4_8	0.4_6	0.3_5	0.4_8
2750		0.6_5	0.4_2	
2650		0.9_1	0.6_7	

4.5 Determination of Transmission for Near-infrared Region

In Sec. 2.3.2, it was indicated that the composite transmission factor, T, for the visible and near-infrared regions of the atmosphere is given by

$$T = T_v(F_v/F) + T_i(F_i/F) \tag{5}$$

So far this report has dealt only with the transmission in the visible region. In order to find the ratios F_v/F and F_i/F in Eq. 5, the effective source temperature must be known. This was another objective of the Thermal Radiation Program at Operation Greenhouse. Table 5 gives the temperatures assigned to the sources as a result of this work. It further indicates the fractional distribution of energy below and above 0.7 μ for each source, assuming a blackbody energy distribution.

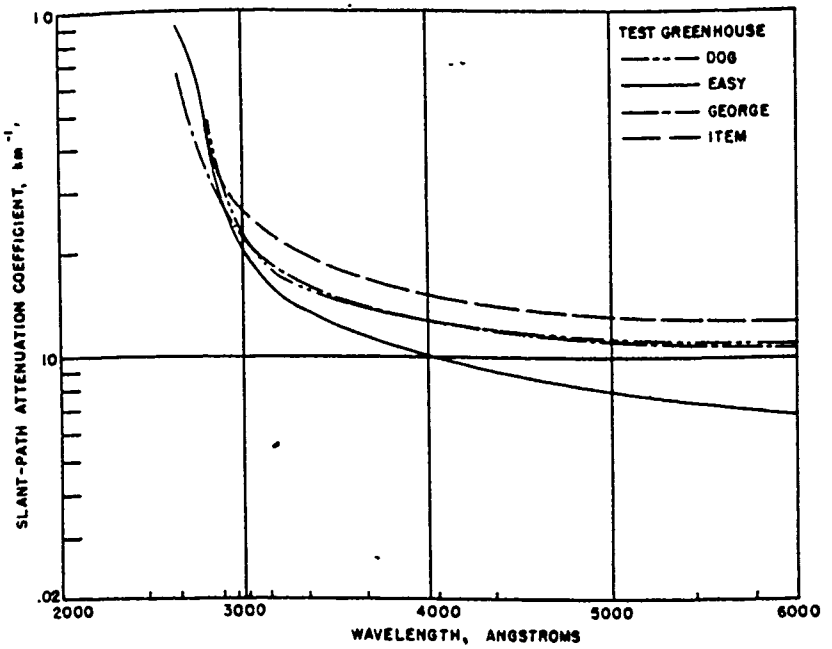

Fig. 9—Slant-path attenuation coefficients vs. wavelength.

TABLE 5—EFFECTIVE SOURCE TEMPERATURE AND PARTITION OF ENERGY BETWEEN VISIBLE AND NEAR-INFRARED REGIONS

Shot	Temp., °K	F_v/F	F_i/F
Dog	4500	0.31	0.69
Easy	4000	0.23	0.77
George	3000	0.08	0.92
Item	4000	0.23	0.77

The problem, then, is reduced to finding T_i. In general, the transmission in the infrared may be given by

$$T_i = 0.7\,\mu \frac{\int J_\lambda T_\lambda \text{ (absorption) } T_\lambda \text{ (scattering) } d\lambda}{0.7\,\mu \int^{\alpha} J_\lambda d\lambda} \qquad (9)$$

where

T_i = transmission factor appropriate for the near-infrared region
J = intensity of emitted radiation at wavelength λ
T_λ (absorption) = transmission per wavelength interval resulting from absorption
T_λ (scattering) = transmission per wavelength interval resulting from scattering

The only extensive information available in the literature as to attenuation by absorption is the selective transmission for "windows" between the absorption bands in the near-infrared.[9]

Thus, in order to make a transmission calculation, the integral in Eq. 9 must be replaced by the summation

$$T_l = \frac{\sum_{n=1}^{8} J_n T_n \text{ (absorption) } T_n \text{ (scattering)}}{\sum_{n=1}^{8} J_n} \tag{10}$$

where n represents the number of "windows" so used in this region.

Unfortunately values for T_n (scattering) are not well known. Calculations have shown that for the clear atmosphere in Nevada one can assume

$$T_\lambda \text{ (scattering)} = T_n \text{ (scattering)} = T_v \tag{11}$$

and have the final corrected flux values close to the values obtained by considering the variation of haze attenuation with wavelength.[10] This assumption was also used for these calculations. Certainly the error introduced here is well within the boundaries introduced by numerous other uncertainties. Hence Eq. 10 becomes

$$T_l = T_v \frac{\Sigma J_n T_n \text{ (absorption)}}{\Sigma J_n} \tag{12}$$

The quantity

$$\frac{\Sigma J_n T_n \text{ (absorption)}}{\Sigma J_n} = T_l \text{ (absorption)}$$

is the total selective transmission for the near-infrared region. This quantity was read from a nomograph found in reference 10, which gives the selective water vapor absorption as a function of source temperature and precipitable water in the path. The pertinent information involved in this determination is given in Table 6.

TABLE 6 — EVALUATION OF THE TOTAL SELECTIVE TRANSMISSION OF WINDOWS BETWEEN WATER VAPOR BANDS IN NEAR-INFRARED REGION

	Dog	Easy	George	Item
Path length, km	3.65 16.3	5.1 32.6	4.4 24.7	5.1 32.6
Ambient air temp., °F	79	79	78	81
Relative humidity, %	78	74	90	64
Water vapor conc., g/m	19.2	18.2	21.2	16.7
Precipitable water per 1000 yd, mm	17.5	16.5	19.4	15.2
Precipitable water per path, mm	58.5 261	77.0 492	78.0 438	70.9 453
Source temp., degrees absolute	4500	4000	3000	4000
T_l (absorption)	0.680 0.582	0.646 0.526	0.60_3 48_9	0.65_2 0.53_3

4.6 Determinations of Effective Transmission

Equation 5 now has the form

$$T = T_v(F_v/F) + T_v\, T_i\ (\text{absorption})\ (F_i/F) \tag{13}$$

The remainder of the calculation is straightforward. Knowing the field of view of each of the thermal flux receivers, the wide field transmission factor, T_v, is computed from the equation

$$T_v = T_v' + 0.5\ (1 - T_v')(1 - e^{-\theta}) \tag{14}$$

which is derived in the article by Stewart and Curcio.[12] In this expression, θ is the angular diameter (in radians) of the field of view of the detecting equipment, T_v' is the narrow-field transmission factor derivable from the attenuation coefficient given in Sec. 4.4, and 0.5 is a geometrical factor which compensates for the amount of the field of view which is actually effective since from ground shots the radiation is only present in half the field. Table 7, then, lists all the information required to determine the composite transmission factor T.

As mentioned earlier, these factors are used in the determination of the amount of thermal energy radiated by the weapons; this is fully discussed in Part II.

TABLE 7—DETERMINATION OF COMPOSITE TRANSMISSION FACTOR T FOR EACH THERMAL FLUX DETECTOR AT EACH SHOT

Shot	Station	Distance, km	Field of view, deg.	Transmission per kilometer	Transmission to station	Transmission with aureole	T_i (absorption)	T_i	F_v/F	F_i/F	$T_v F_v/F$	$T_i F_v/F$	Composite factor, T
	M	3.66	15		0.666	0.705	0.680	0.479			0.218	0.331	0.549
			15		0.666	0.705	0.680	0.479			0.218	0.331	0.549
Dog	Parry	16.3	3	0.895	0.164	0.185	0.582	0.107	0.31	0.69	0.057	0.074	0.131
			10		0.164	0.231	0.582	0.134			0.072	0.092	0.164
			20		0.164	0.287	0.582	0.167			0.089	0.115	0.204
	P	5.1	17		0.687	0.727	0.646	0.469			0.167	0.361	0.528
			17		0.687	0.727	0.646	0.469			0.167	0.361	0.528
Easy	Parry	32.6	3	0.929	0.091	0.114	0.526	0.060	0.23	0.77	0.026	0.046	0.072
			10		0.091	0.164	0.526	0.086			0.038	0.066	0.104
			20		0.091	0.225	0.526	0.118			0.052	0.091	0.143
			24		0.091	0.247	0.526	0.130			0.057	0.100	0.157
	N	4.4	17		0.605	0.656	0.603	0.396			0.052	0.364	0.446
			17		0.605	0.656	0.603	0.396			0.052	0.364	0.446
George	Parry	24.7	3	0.892	0.059	0.083	0.489	0.041	0.08	0.92	0.007	0.038	0.045
			10		0.059	0.135	0.489	0.066			0.011	0.061	0.072
			20		0.059	0.197	0.489	0.096			0.016	0.088	0.104
	P	5.1	20		0.583	0.644	0.652	0.419			0.148	0.323	0.471
			20		0.583	0.644	0.652	0.419			0.148	0.323	0.471
Item	Parry	32.6	3	0.896	0.032	0.057	0.533	0.030	0.23	0.77	0.013	0.023	0.036
			19		0.032	0.168	0.533	0.089			0.039	0.068	0.107
			25		0.032	0.203	0.533	0.108			0.047	0.083	0.130

5 CONCLUSIONS

Prior to Operation Greenhouse total thermal measurements had been made at several nuclear weapons tests. Although the data gathered were good, it was obvious that a reasonable knowledge of atmospheric attenuation was necessary in order to evaluate correctly the data taken. Thus these measurements were made at Operation Greenhouse. Furthermore, knowledge of the process of atmospheric attenuation over the spectral range of which we are concerned is

increasing all the time. An attempt has been made in this report to bring the results from the data originally taken into agreement with the present level of understanding of the processes involved in atmospheric attenuation. It is felt that the results given here are the best possible with the information available at the present time.

It should be noted that the main result of this better appreciation of atmospheric transmission is a realization that the effective attenuation is more pronounced than originally thought. The net result is a lower transmission factor and, consequently, greater apparent thermal yield from the nuclear explosions.

Appendix 1: Theoretical Justification for Indirect Method of Determination of Slant-path Transmission

Let us first consider a simple development for the determination of slant-path transmission from total thermal measurements. This development, as will be seen, is open to question; but posing and answering questions about it leads to a better presentation. This oblique approach is deliberate. It is used in order to clarify the importance of the various parameters involved and to indicate the nature of several important assumptions.

From total thermal measurements made at, say, stations N and P, values of the flux received are given as F_N and F_P. Now,

$$F_N = \frac{T_N J}{4\pi D_N^2} \tag{15}$$

where T_N is an average transmission value over the measured spectrum, J is the energy emitted by source, and D_N is the distance of source from station N.

Likewise

$$F_P = \frac{T_P J}{4\pi D_P^2} \tag{16}$$

Dividing Eq. 16 by 15,

$$\frac{F_P}{F_N} = \frac{T_P}{T_N}\frac{D_N^2}{D_P^2} = \frac{e^{-\alpha D_P}}{e^{-\alpha D_N}}\left(\frac{D_N}{D_P}\right)^2 \tag{17}$$

where, having applied Lambert's attenuation law, α is an average attenuation coefficient for the slant path over all wavelengths. Rewriting,

$$\frac{F_P}{F_N} = e^{\alpha-(D_P-D_N)}\left(\frac{D_N}{D_P}\right)^2 \tag{18}$$

From this expression α can be determined, all other quantities being known.

The following objections to the possibility that this α is equivalent to the α measured by the telephotometer are given:

(a) Measurements of total thermal energy are made through the near-infrared region. The equation set up above for computing α for the visible region assumes an exponential function for varying distances (Lambert's law). This is not necessarily true in the near-infrared.

(b) The telephotometer α is for a specific wavelength (α_{λ_1}) whereas the α computed above is an average value over all wavelengths ($\alpha_{\lambda av.}$). Therefore they should not necessarily be in agreement.

(c) The slant path measured by the α above is not the same slant path measured by the telephotometer.

Notwithstanding the truth of (a), the assumption of an exponential dependency was still used in lieu of a better one. The check mentioned in Sec. 2.4 served to indicate that within the accuracy of known facts the assumption was a reasonable one.

To answer (b), set up the energy as a function of wavelength.

$$J = \int_0^\infty J_\lambda d\lambda \tag{19}$$

At a distance D, the energy received is

$$F_D = \frac{1}{4\pi D^2} \int_0^\infty J_\lambda e^{-(\text{slant } \alpha_\lambda)D} \, d\lambda \tag{20}$$

For stations N and P, then

$$F_N = \frac{1}{4\pi D_N^2} \int_0^\infty J_\lambda e^{-(\text{slant } \alpha_\lambda)D_N} \, d\lambda \tag{21}$$

$$= \frac{e^{\beta D_N}}{4\pi D_N^2} \int_0^\infty J_\lambda e^{-(\text{horizontal } \alpha_\lambda)D_N} \, d\lambda \tag{22}$$

and

$$F_P = \frac{e^{\beta D_P}}{4\pi D_P^2} \int_0^\infty J_\lambda e^{-(\text{horizontal } \alpha_\lambda)D_P} \, d\lambda \tag{23}$$

where use has been made of the relation between slant α_λ and horizontal α_λ, i.e., β = horizontal α − slant α.

By dividing Eq. 23 by Eq. 22

$$\frac{F_P}{F_N} = \left(\frac{D_N}{D_P}\right)^2 e^{\beta(D_P - D_N)} \; \frac{\int_0^\infty J_\lambda e^{-(\text{horizontal } \alpha_\lambda)D_P} \, d\lambda}{\int_0^\infty J_\lambda e^{-(\text{horizontal } \alpha_\lambda)D_N} \, d\lambda} \tag{24}$$

and assuming a black-body temperature for the bomb, β can be determined. This expression takes into account the change in α with wavelength.

Objection (c) is also answered by Eq. 24 because horizontal α_λ is independent of the length of the horizontal path measured. Thus, regardless of the length of slant path measured, as long as it is to the same elevation and one can make the assumption that the atmosphere is composed of horizontal strata, the value of slant-path transmission will remain the same.

Lastly, since β in Eq. 24 is independent of wavelength, this β is equivalent to the β determined by telephotometer measurements.

Appendix 2: Densitometry Records for Atmospheric Transmission

TABLE 8—DENSITOMETRY RECORD FOR ATMOSPHERIC TRANSMISSION, SHOT DOG PLATES K7 AND K8, APR. 8, 1951

Values Given are Percent Transmission of Photographic Plate

λA	Spectrograph	Exposure time = 15 min Step Wedge					Exposure time = 3 min				
		5	4	3	2	1	5	4	3	2	1
5780	Distant	87	32	3.0				90	44	3.2	
	Close	71	14					75	15.2	0.9	
5460	Distant	90	40	4.9				93	52	5.3-5.6	
	Close	82	22	0.9				85	26	1.9	
4360	Distant	76	24	2.1				80	27	2.6	
	Close	65	12.5					66	13	1.1	
4050	Distant	84	36	6.2				85	39	7.1	
	Close	73	25	2.5				74-76	25	4.1	
3660	Distant	41	9.4	1.4			84	41	10	1.7	
	Close	37	7				81	35	7.2	1.4	
3340	Distant		79	45	18.5	2.4			85	50	11.5
	Close		79	39	15.5	2.2			79	49	12
3130	Distant	66	30.5	10	3.0		96	68	33	11.5	2.0
	Close	77	37.5	11.3	3.6			74	36.5	15	3.1
3020	Distant	87	54	23	7.4	1.2		86	52	22	4.6
	Close	95	66	29	10.5	1.8		95	60	36	9.0
2970	Distant	97	75	41	16	3.2		96	74	40	10
	Close		88	56	26	5.7			91	64	23
2890	Distant		89	66	36	9.4			95	71	29
	Close			95	73	29				95	65
2805	Distant		77	46	20	4.0			84	49	15
	Close				87	45					81

TABLE 9—DENSITOMETRY RECORD FOR ATMOSPHERIC TRANSMISSION, SHOT ITEM PLATES R6 AND R8, MAY 25, 1951

Values Given are Percent Transmission of Photographic Plate

λ(A)	Spectrograph	Exposure time = 15 min Step Wedge					Exposure time = 3 min					Exposure time = 1 min				
		5	4	3	2	1	5	4	3	2	1	5	4	3	2	1
5780	Distant	83	37	5.6				90	45	6.4				85	31	
	Close	65	16					71	14	1.1			92	50	9.5	
5460	Distant	89	46	7.8-8.4				92	54	9.1				87	41	1.3
	Close	74	23	1.5				77	21	1.9			95	60	14	
4360	Distant	76	29	3.8				79	32	4.5			95	71	22	
	Close	60	15				94	59	11	1.0			87	38	7.4	
4050	Distant	84	41	11	1.3			85	44	11			97	78	34	2.4
	Close	72	27	3.8				70	23	4.5			90	52	18	
3660	Distant	48	15	3.1			83	45	15	3.2			74	35	10	9-1.0
	Close	41	11	1.6			75	36	9.0	1.8			63	23	6.5	
3340	Distant		80	53	25	5.4			82	54	17			96	77	34
	Close		82	46	23	4.8			78	50	15			93	74	31
3130	Distant	71	39	16.5	6.1	1.2	92	68	38	16	3.4		87	59	31	8.6
	Close	75	44	17	6.7	1.5		72	39	18	4.2		90	61	35	10.5
3020	Distant	88	60	30	13	3.0		86	58	29	7.4			78	50	18
	Close	95	71	36	16	4.2		95	68	38	12.5			85	59	25
2970	Distant	96	77	48	23	6.2		95	76	46	14			92	72	31
	Close		89	59	32	9.8			86	60	26			95	81	44
2890	Distant		93	73	45	16			94	74	33				90	57
	Close			91	70	32				93	61					80
2805	Distant		82	54	27	7.8			84	55	20			94	76	37
	Close			94	76	39				96	70					88

TABLE 10—DENSITOMETRY RECORD FOR ATMOSPHERIC TRANSMISSION, SHOT GEORGE PLATES P3 AND P4, MAY 9, 1951

Values Given are Percent Transmission of Photographic Plate

λ(A)	Spectrograph	Exposure time = 15 min Step Wedge					Exposure time = 3 min					Exposure time = 1 min				
		5	4	3	2	1	5	4	3	2	1	5	4	3	2	1
5780	Distant	90	44	7-8				91	54	8.2				89	41	1.0
	Close	58	9.1				95	55	7.2				91	38	4.3	
5460	Distant	93	56	12				95	66	13				94	51	2.0
	Close	67	13				97	66	13				95	50	6.7	
4360	Distant	81	35	5.5				83	39	6.3				79	29	1.2
	Close	53	8.3				91	45	6.4				82	28	3.7	
4050	Distant	86	48	14	1.8			87	53	15				84	42	4.2
	Close	65	19	2.0			92	58	16	2.4			86	43	11	
3660	Distant	51	17	3.7			85	50	18	4.4		98	76	40	13	1.5
	Close	32	6.6				68	27	5.6	1.2		92	51	16	3.8	
3340	Distant		85	56	28	6.4			86	59	22			96	81	39
	Close		76	41	18	3.2		95	73	44	11			91	65	23
3130	Distant	74	42	19	6.8	1.4	94	73	43	20	5.0		90	64	36	11
	Close	73	36	13	4.8	1.0	93	66	33	14	3.0		86	51	25	6.2
3020	Distant	89	62	33	14	3.4		88	64	35	11			82	54	22
	Close	89	61	29	12	2.6		86	57	30	8.0			79	49	17
2970	Distant	97	79	50	25	7.4		97	81	52	21			93	73	36
	Close		81	50	24	6.4		97	81	52	20			95	73	33
2890	Distant		94	76	47	17			94	78	41				92	61
	Close		97	82	56	21			97	83	47				96	67
2805	Distant		82	54	29	8.9			82	57	25			94	77	40
2750	Close			79	52	19				81	43				94	63
2650	Distant	92	70	41	19	5.4		92	72	44	16			88	64	29.5
	Close			96	82	44				96	75					90

TABLE 11—DENSITOMETRY RECORD FOR ATMOSPHERIC TRANSMISSION, SHOT EASY PLATES M7 AND M8, APR. 21, 1951

Values Given are Percent Transmission of Photographic Plate

λ(A)	Spectrograph	Exposure time = 15 min Step Wedge					Exposure time = 3 min					Exposure time = 1 min				
		5	4	3	2	1	5	4	3	2	1	5	4	3	2	1
5780	Distant	86	42	7.0				89	52	6.8				87	37	0.9
	Close	48	6.2				91	51	5.2				85	30	2.4	
5460	Distant	90	53	11				92	61	11				88	46	1.6
	Close	55	9.2				93	61	8.6				88	39	4.3	
4360	Distant	79	33	4.6				82	39	5.8			93	74	25	
	Close	44	6.3				87	43	5.2				77	24	2.6	
4050	Distant	84	46	12	1.4			85	50	13			94	77	37	3.0
	Close	57	15	1.2			91	58	13	1.8			82	38	8.8	
3660	Distant	52	17	3.4			84	50	18	4.0		96	74	38	11	1.0
	Close	30	5.6				65	25	4.4			87	49	14	2.8	
3340	Distant	96	82	55	28	6.3			84	59	21			95	78	38
	Close	92	68	35	13	2.0		90	67	37	9.2			86	59	19
3130	Distant	73	41	18	6.0	1.3	94	72	44	20	4.8		87	62	34	10
	Close	66	33	11	3.8		90	63	31	13	2.8		83	50	23	5.6
3020	Distant	88	63	34	14	3.0		86	62	35	10		94	79	51	20
	Close	86	58	26	10	2.2		84	55	29.5	8		97	76	47	15.5
2970	Distant	93	77	50	24	6.4		94	78	52	19			89	70	33
	Close	96	80	49	23	5.9		96	79	52	20			91	72	33
2890	Distant		93	75	49	17			93	77	40				90	57
	Close		97	85	62	25				87	55				97	73
2805	Distant	95	82	56	30	8.1			82	60	24			92	74	39
	Close			92	74	38				92	68					84
2750	Distant		92	81	59	24				85	52				94	69
	Close					87										
2650	Distant	90	69	41	18	4.9		92	71	45	16			87	61	29
	Close					94										

REFERENCES

1. J. A. Curcio et al., An Experimental Study of Atmospheric Transmission, J. Opt. Soc. Am., 43: 97(1953).
2. C. A. Pearson, A Recording Atmospheric Transmissometer, Report NRL-3949, Naval Research Laboratory, March 1952.
3. Lord Rayleigh, On the Scattering of Light by Small Particles, Phil. Mag., 41: 447(1971): "Scientific Papers," Vol. 1, pp. 104-110, Cambridge Press, London, 1899; On the Transmission of Light through An Atmosphere Containing Small Particles in Suspension, Phil. Mag., 47: 375(1899): "Scientific Papers," Vol. 4, pp. 397-405, Cambridge, London, 1903.
4. J. A. Stratton and H. G. Houghton, A Theoretical Investigation of the Transmission of Light through Fog, Phys. Rev., 38: 159(1931).
5. L. Dunkelman, Horizontal Attenuation of Ultraviolet and Visible Light by the Lower Atmosphere, Report NRL-4031, Naval Research Laboratory, September 1952.
6. J. N. Howard, The Absorption of Near-Infrared Blackbody Radiation by Atmospheric Carbon Dioxide and Water Vapor, Ohio State University Research Foundation Project 407, Report No. 1, March 1950.
7. H. A. Gebbie et al., Atmospheric Transmission in the 1-14μ Region, Proc. Roy. Soc., A206: 87(1950).
8. H. S. Stewart et al., Greenhouse Report NRL-H No. B51, Vol. VII, Appendix A, January 1951.
9. T. Elder and J. Strong, The Infrared Transmission of Atmospheric Windows, J. Franklin Inst., 255: 189(1953).
10. L. F. Drummeter, A Method for Estimating Total Atmospheric Transmission of the Nevada Atmosphere, Report NRL-4379, Naval Research Laboratory, April 1954 (Classified).
11. H. W. Yates, Total Transmission of the Atmosphere in the Near Infrared, Report NRL-3858, Naval Research Laboratory, September 1951.
12. H. S. Stewart and J. A. Curcio, The Influence of Field of View on Measurements of Atmospheric Transmission, J. Opt. Soc. Am., 42: 801(1952).

Part II
Total Thermal Radiation

Radiometry Branch, Optics Division
Naval Research Laboratory
Washington, D. C.

April 1959

ABSTRACT

The radiant energy incident at several observing stations was measured during each of the four explosions at Operation Greenhouse with thermopiles sensitive in the wavelength interval 0.23 to 12 μ. The outputs of the thermopiles were recorded ballistically with recording galvanometers.

PREFACE

This report describes the measurement of total thermal radiation from nuclear weapons carried out at Operation Greenhouse by the Radiometry Branch of the Optics Division, U. S. Naval Research Laboratory, for the Los Alamos Scientific Laboratory. The work was carried out under the direction of Harold S. Stewart and was part of the over-all program of measurements carried out under the general supervision of Wayne C. Hall.

The measurements at the two-mile stations were the responsibility of Louis F. Drummeter; those made at Parry Island were carried out by Joseph A. Curcio and John A. Sanderson.

The original manuscript for this report was prepared by Edward M. Man. Minor revisions of the data presented in the original manuscript and final technical editing were performed by D. F. Hansen and J. H. Campbell.

1 OBJECTIVE

One of the objectives of the Thermal Radiation Program at Operation Greenhouse was to determine the total thermal yield of each of the nuclear weapons tested. The bulk of the thermal energy was considered to be emitted in wavelengths between 0.23 μ in the ultraviolet and 12 μ in the infrared.

The determination of the total thermal energy was undertaken as a three-step process. Step one involved the determination of the total thermal energy incident at an observing station located a known distance from the weapon. Step two involved the determination of the attenuation of the radiation by the atmosphere between the observing station and the bomb. Step three consisted of the correction of the measured flux by means of the atmospheric attenuation in order to determine the vacuum flux incident at the station and thus the total thermal energy radiated by the explosion.

Under step one the thermal energy was measured by means of radiation thermopiles which were uniformly black for all wavelengths of thermal radiation. For each shot, measurements were made at two distances. One observing station was located at Parry Island, a distance of from 8 to 20 miles from the various explosions. The other station was a nominal two miles from the weapon. At least two observations were made at each station.

A separate project was established to determine the transmittance of the atmosphere in the wavelength region of interest, step two. This project is described in detail in Part I of this report. Another assessment of atmospheric transmittance was obtained by comparing data recorded at the near, two-mile, station with that recorded at the remote station on Parry Island.

Step three is to be accomplished in this report.

2 BACKGROUND

Prior to Operation Greenhouse total thermal measurements had been made at Trinity and at Operations Crossroads and Sandstone. The measurements of Trinity were made by Williams and Yuster of the Los Alamos Scientific Laboratory.[1] For the latter two operations, the measurements were made by the Optics Division, Naval Research Laboratory, by Sanderson and Stewart at Operation Crossroads[2] and by Richardson and Butler at Operation Sandstone.[3]

TABLE 1—SUMMARY OF TOTAL THERMAL YIELD DETERMINATIONS FOR TESTS PRIOR TO OPERATION GREENHOUSE

	Trinity	Crossroads, Able	Sandstone, Yoke	Sandstone, Zebra
Apparatus used	Thermopile, photographed meter	Spectrograph (0.32 to 0.86 μ)	Thermopile	Thermopile
Range, km	9.1	32.9	24.7	16.3
Radiant energy incident per unit area (uncorrected), ergs/cm^2	1.22×10^7	5×10^5	2.3×10^6	3.35×10^6
Total thermal energy radiated (without atmospheric correction), ergs	1.3×10^{20}	6.8×10^{19}	1.8×10^{20}	1.1×10^{20}
Atmospheric transmittance (for range)		0.055	0.20	0.33
Total thermal energy radiated (corrected), ergs	1.3×10^{20}	9.7×10^{20}	9.0×10^{20}	3.3×10^{20}
Total thermal yield (corrected), kt	3.1	23	22	7.9
Radiochemical yield of bomb, kt	23.8	22.0	48.7 ± 2.4	18.2 ± 0.9

Table 1 summarizes the results of the measurements prior to Operation Greenhouse. There were no direct measurements of atmospheric transmittance made during these three operations. Thus the results obtained at Trinity are the most reliable because the measurements were made under conditions for which the effects of light scattering and transmittance

of the atmosphere did not introduce serious errors. In fact, the total thermal yield is probably only about 15 per cent below the value which would have been obtained if adequate transmittance and scattering corrections had been made.

The atmospheric transmittance corrections for Operations Crossroads and Sandstone were calculated by taking into consideration the estimated spectral energy distribution of the source. The Operation Crossroads data were treated by the investigators as though the source radiated with a spectral energy distribution appropriate to a black body of temperature in excess of [illegible]. The Operation Sandstone data were corrected by using a transmission factor appropriate to a source of temperature approximately [illegible].

As may be seen in Table 1, the observations at Operations Crossroads and Sandstone were made at ranges in excess of 10 miles. The basic measurements of flux of radiation reaching the instruments are quite reliable. However, the thermal yields obtained from these measurements are inaccurate because long-range optical observations are subject to two types of error. One type of error involves the effect of the field of view of the detecting equipment; the other involves the temperature assigned to the explosion.

The effect of field of view on the energy received by a detector is discussed in reference 4. The results presented there indicate that, for clear weather, the correction for field of view is small when the distance from source to receiver is of the order of two miles but can be large for distances of 10 miles or more. For example, at a distance of 15 miles in a clear atmosphere (visibility of 20 miles), it is quite possible that measurements made with a 25-degree field of view and a 3-degree field of view will differ by a factor of 2.

Atmospheric attenuation also changes with wavelength; thus, if the spectral energy distribution assigned to the radiation from the explosion is incorrect, the correction for atmospheric attenuation will be inaccurate. The effect of this kind of error increases rapidly with distance.

3 INSTRUMENTATION

3.1 Theory Behind Instrumentation

The thermal radiation emitted by an atomic bomb explosion is similar to that from a black body, whose temperature varies between [illegible] throughout the time when radiation is emitted, the exploding surface is blanketed by an attenuating medium sufficient to block almost all black-body radiation below 0.29 μ. The purpose of these investigations was to determine the total thermal energy received at various distances from an explosion without regard to the distribution of this energy in wavelength or in time. To achieve this result, blackened thermopiles which were equally sensitive at all wavelengths between 0.23 and 12 μ were used as detectors; the electrical output of each thermopile was connected to a galvanometer and the deflection of the galvanometer recorded on moving paper tape.

The fundamental equation which describes the response of a thermopile-galvanometer system such as that used here is given by

$$\frac{1}{k}\int_0^\infty \theta_t \, dt = \int_0^\infty F_t dt \qquad (1)$$

where θ_t is the angular deflection of the galvanometer at time t; F_t is the radiant thermal energy, in watts/cm^2, incident on the thermopile at time t; and k is the sensitivity constant of the thermopile-galvanometer system determined for a steady state of indication. The time constant of this thermopile-galvanometer system was of the order of 5 sec. The area under the deflection curve is proportional to the energy incident on the thermopile and was used to evaluate the total radiant energy incident at various distances from the explosion.

In order to compute from the measured values of radiant energy incident per unit area the total thermal radiation emitted by each explosion, it was necessary to know the effective specular transmittance of the atmosphere for thermal radiation and to correct this specular trans-

mittance for the field of view, or aureole, effect of the measuring instrument (see reference 4). The method for obtaining atmospheric transmission values and the results of measurements for the Operation Greenhouse shots are given in Part I. A brief description of the method is repeated here.

Correction for the effect of atmospheric transmission on the thermal yield measurement can only be made when the spectral distribution of the energy received by the thermopile and the spectral transmittance of the intervening atmosphere are known. This information was available from data taken at the two-mile stations by high-speed spectrographs.[5] The response of the high-speed spectrograph was limited to the wavelength interval 0.23 to 0.7 μ. Above these wavelengths, the spectral energy distribution of the radiation received at the two-mile stations was assumed to be that which would be emitted by a black body whose energy distribution would account for the envelope of the spectrum obtained. It was not necessary to know the absolute values of the energy received by the spectrograph; only the relative values versus wavelength were required for this correction.

Spectral transmittance measurements were made over a horizontal path between Parry and Eniwetok Islands at H – 1 hr for each shot. In addition, a recording photoelectric transmissometer was operated over a slant path from shot-tower cab to ground station for Dog and Easy shots.

The attenuation coefficient obtained for the slant path was lower than that measured over the horizontal path for the same wavelength. The higher attenuation over the horizontal path was assumed to be caused by nonselective scattering from large particles close to the water surface. This effect is constant for each wavelength; thus, for the Dog and Easy shots, each horizontal-path coefficient was adjusted by the same amount to give appropriate slant-path spectral attenuation coefficients.

On the George and Item shots, no slant-path transmissometer data were available; therefore it was necessary to arrive at the slant-path transmittance in an indirect manner. The method used was tested with values from the Dog shot transmittance data and shown to give correct results. The final report for all shots is a composite transmittance figure which is used in this report to give the true thermal yield values.

3.2 The Eppley Thermopiles

The sensitive elements which detected the radiation were Eppley circular thermopiles. These rugged, relatively insensitive, commercial thermopiles are constructed by cementing four copper-constantan thermoelectric junctions (see Fig. 1) to one side of a thin copper disk, 5.4 mm in diameter, the other side of which was heavily coated with lampblack to absorb radiation incident on it. The time constant of each thermopile was approximately 3 sec and the resistance about 4 ohms.

Each thermopile was enclosed in a sturdy housing as shown in Fig. 2. A circular aperture, 6.9 mm in diameter, in the front wall of the housing admitted radiation to the thermopile. This aperture was closed by an optical window of lithium fluoride 1 mm thick and transparent throughout the spectral interval of 0.2 to 12 μ.

3.3 Recording Galvanometer

Each thermopile was connected directly to a General Electric recording flux meter modified to permit its use as a recording galvanometer. This instrument had as a sensitive element a taut suspension galvanometer with response time of 3.5 sec. The coil resistance was in the neighborhood of 13 ohms, and the external critical damping resistance was about 30 ohms for each of the several instruments. When connected with the 4-ohm thermopiles the galvanometers were over-damped, resulting in time constants for the complete thermopile-galvanometer system of the order of 5 sec.

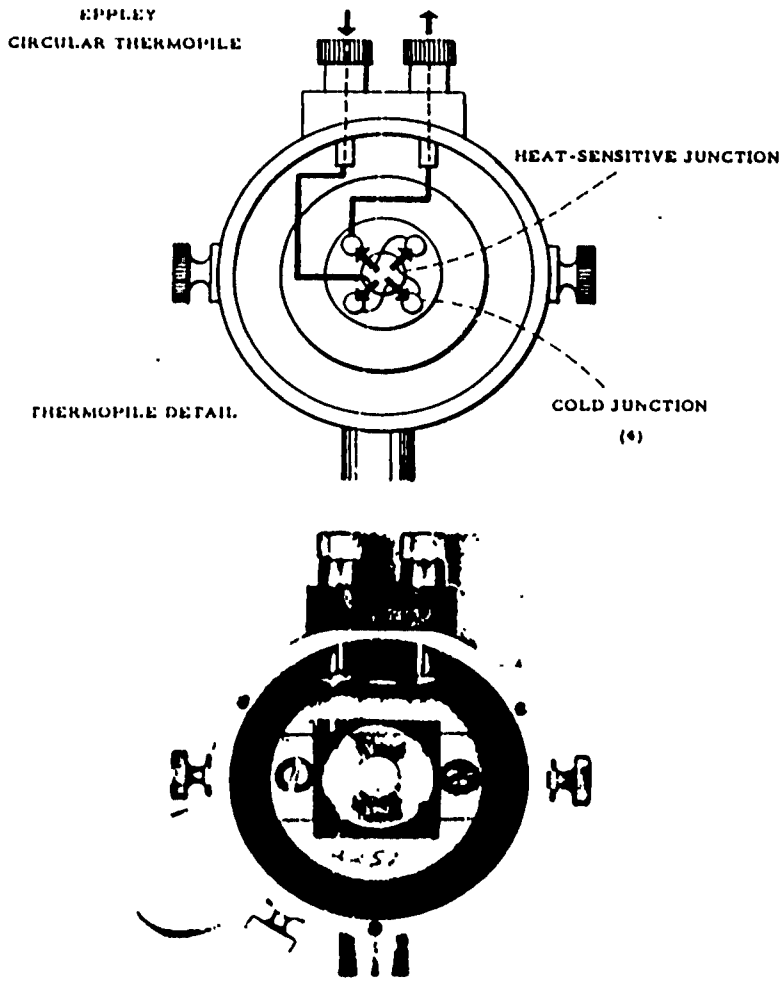

Fig. 1 — Details of thermojunctions contained in the Eppley thermopile.

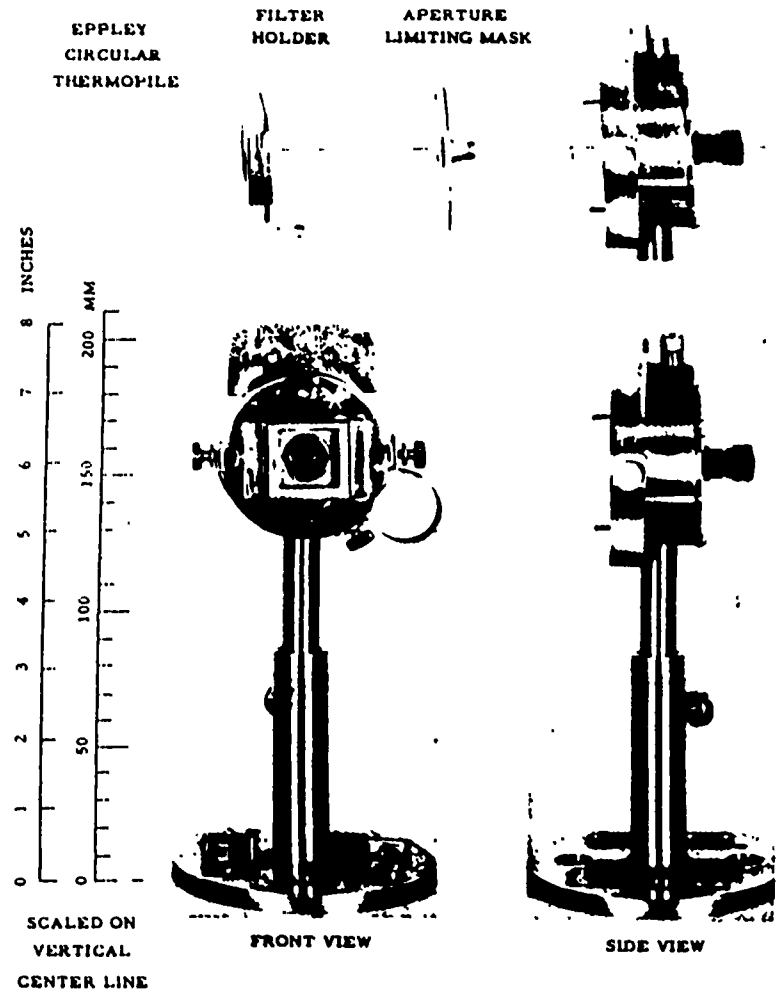

Fig. 2 — The Eppley circular thermopile.

The General Electric flux meter included a photoelectric system which amplified and recorded deflections of the primary galvanometer. The galvanometer deflection controlled the relative intensities of light from a bright tungsten lamp reaching two photocells connected in opposition. Resulting photoelectric current was amplified and used to drive a rugged recording pen which wrote on moving paper. Paper speeds of 0.05 and 0.10 in./sec were used.

3.4 Calibration of the Thermopile-Galvanometer System

The data presentation from the thermopile-galvanometer system were a curve on recording paper showing the galvanometer deflection as a function of time. (See Fig. 3). It was necessary to obtain from such curves the total thermal energy incident on the thermopile.

The first step in the interpretation of these curves was to reproduce them on a rectilinear plot by obtaining time from known rate of paper travel (dependent upon the synchronous drive motor of the recorder for constancy of speed) and by converting meter deflection to microamperes, using a carefully measured current versus deflection calibration curve for the particular instrument. The departure from linearity of response of the recorders was not large but a correction for it was required.

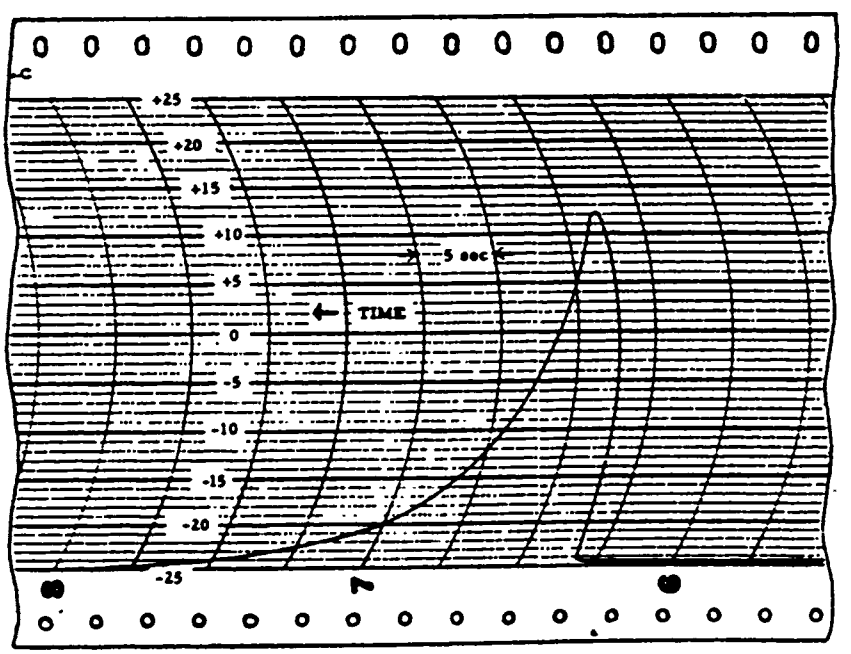

Fig. 3—Typical trace from a thermopile-galvanometer recorder system.

It was convenient to plot each record to the same scale of coordinates and, therefore, to express the calibration constant of the system in terms of joules/cm^2 per unit area of record. Thus

$$Q = \int_0^\infty F_t\,dt = CA, \text{ joules/cm}^2 \qquad (2)$$

where Q is the calibrating exposure, C is the calibration constant, and A is the area under the curve. Since A also represents the product, microamperes times seconds, it is less arbitrary to express C in joules/cm^2 per microampere-second. The next step is the determination of C.

A 500-watt tungsten projection lamp was carefully calibrated by reference to a National Bureau of Standards radiation standard. Hence irradiance at a known distance from the lamp was easily determined. A thermopile, connected to the General Electric recording galvanometer with which it was to be associated in the actual test, was placed a known distance from the secondary standard lamp. The thermopile received light from the lamp in a manner which excluded reflected or scattered rays. Also, to eliminate from the light path the infrared radiation produced by the heating of the glass envelope, a $\frac{1}{4}$-in.-thick glass plate was introduced into the light path.

An opaque shutter, which could be removed and replaced quickly, was used to expose the thermopile to a constant irradiance (F_0) successively for periods of 5, 10, and 20 sec, giving three separate recordings of deflection as a function of time for total exposures given by $Q = F_0 t$ joules/cm^2. These recordings were reduced to rectilinear plots. (See Fig. 4.) The area

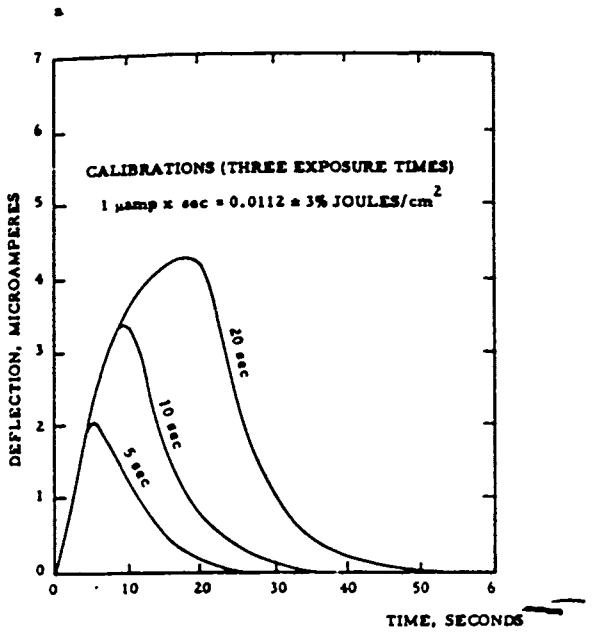

Fig. 4—Typical standard lamp calibration record

under each of these three curves was determined by use of a planimeter and expressed in microampere-seconds. Since the radiation incident on the thermopile was known and the time of exposure fixed, from Eq. 1 the total radiation per unit area incident on the thermopile was known. (A check on the consistency of results was possible at that time since the ratio of flux for the three exposures should be 1 : 2 : 4.) Therefore from Eq. 2 the calibration constants for the system could be determined.

3.5 Scaling to the Expected Yield

It was necessary to make a pretest estimate of the total integrated flux density that would fall on each thermopile by evaluating the expected total yield of the bomb and expected atmospheric transmission. Then, where necessary, the sensitivity of each thermopile was adjusted so that the recorder would stay on scale for the shot.

The following procedure was used. The thermopile was exposed to the secondary standard source for 20 sec and the characteristic rise curve obtained. The shutter was then closed, and the decay curve recorded. The conditions of illumination were so chosen that the maximum

deflection at 20 sec was well up toward full scale of the recorder. The decay curve was then extrapolated back to full-scale deflection, and a vertical line, displaced about 1 sec toward zero time, was dropped down to the time axis. The area under the new curve and the solid section of the decay curve represent approximately the ballistic response of the system to a square pulse of radiation 1 sec in duration. The displacement of the vertical line by 1 sec toward zero time was an arbitrary expression of the experimenter's judgment of the similarity between such a square pulse and a real explosion. The area under this curve, interpreted as joules per square centimeter, therefore represented the total integrated radiant energy per unit area which would produce full-scale meter deflection.

This procedure was followed with each thermopile-galvanometer system. It was a conservative procedure, for it was known that the square-pulse approximation represented a faster rate of delivery of energy to the system than would exist in reality.

It may be noted that the time constant of the system used to produce the curves shown in Fig. 4 was about 5.5 sec as derived by measuring the time required for the system to fall from maximum deflection to 1/e of that value. It is also noted that precise knowledge of the time constant is not required; it is only convenient that the time constant be large with respect to the time during which energy is released by the explosion.

Having determined the maximum safe integrated flux density for each thermopile, it was necessary to make the best estimate possible of the maximum and minimum integrated flux densities which would reach the thermopile through the atmosphere. This was done by making certain gross assumptions about atmospheric transmission and thermal yield. Maximum and minimum attenuation coefficients were estimated from day-to-day transmissometer data from which a considerable experience in maximum and minimum excursions developed. It was also assumed that one-third of the expected weapon yield would be manifested as thermal energy. Then, from the equation

$$\int_t^\infty F_t\,dt = \frac{1}{3}\,\frac{WT}{4\pi R^2} \tag{3}$$

where W = total expected energy yield of the bomb, in joules
T = assumed value of atmospheric transmittance
R = range from thermopile to explosion, in cm

the estimated value of flux to be received from the explosion was obtained. This value was compared with the maximum signal recordable by the thermopile system, and any required reduction in sensitivity thus determined. If a reduction in sensitivity was required, it was achieved by mounting a secondary aperture centrally over the thermopile window and very near to it, as shown in Fig. 2.

The transmission coefficient of this aperture was measured directly by observation of thermopile response to a source of radiation with and without the aperture in place. For apertures of moderate diameter, a thermopile system could be calibrated directly with the aperture in place. For very small apertures, however, it was necessary to calibrate the fully exposed thermopile and to determine independently the transmission coefficient of the aperture. Values ranged between 0.67 and 30 per cent for instruments used at various distances and for various predicted yields.

4 RESULTS

Two thermopile-galvanometer systems were used for each test at stations approximately two miles from the explosion. The distances varied from test to test and are given in Table 2. (Three, and on one occasion four, thermopiles were used at Parry Island for each test.) All total thermal stations and their locations relative to the shots are shown in Fig. 5 of Part I.

The results obtained at the two-mile stations were more important to the fundamental measurements of thermal yield than those obtained at the Parry Island station. Atmospheric

attenuation was less severe over the short path than over the longer path. Also, the aureole effect was smaller because of the high transmission over the short path. In two instances thermopiles were arranged so that one viewed the entire fireball with a field of view of about 15 degrees and another viewed only the upper half of the fireball. This was accomplished by locating the cab at the top of the tower precisely in the center of the field of view with the lower half of the field blocked off by a sheet of metal located about 40 cm in front of the thermopile. The installation of thermopiles at site M is shown in Fig. 5. The obstructing plate across the lower half of the field of view of the right-hand thermopile can be seen.

The thermopiles at Parry Island were arranged to have circular fields of view of 3, 10, 20, and, on the fourth time, 24 degrees, by the simple expedient of mounting them 40 cm behind circular apertures 2, 7, and 14.1 cm in diameter, respectively. The 24-degree field of view was realized with an unobstructed thermopile, the housing of which provided the limiting aperture. In addition to the thermal data, useful information on the effect of field of view on the total flux received was obtained from this arrangement of thermopile systems.

On Parry Island at shot Easy, three of the thermopiles were operated with General Motors d-c breaker type amplifiers. This was an expediency resulting from unavailability of a sufficient number of General Electric recording microammeters for this particular event. While this type of amplifier is excellent, corrosion or other difficulties were present in the three available units, and the results obtained were not reliable, as noted in the tables of data.

The values of total thermal energy received at the various stations are presented in Table 2; also given in the table are the ranges from each station and fields of view for each thermopile.

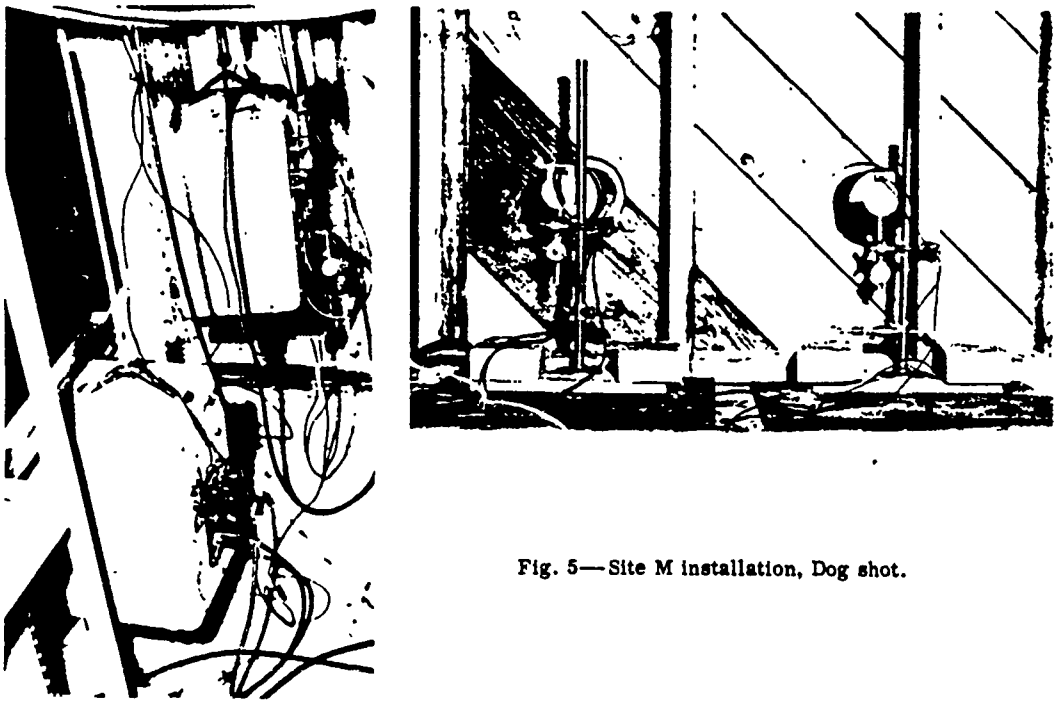

Fig. 5—Site M installation, Dog shot.

Table 3 shows the results of correcting the thermopile measurements for atmospheric transmission and relating the result back to the total thermal yield of the weapon. The total thermal yield (W) is thus given by

$$W = \frac{4\pi R^2 E}{T} \text{ joules} \qquad (4)$$

where E = incident energy at the thermopiles, in joules/cm^2, and T = composite thermal transmittance (from Part I).

Total thermal and radiochemical yields are compared in Table 4. The mean value of total thermal yield for each shot was used. The ratios of total thermal yield to radiochemical yield are formed. An average value of total thermal radiation equal to [redacted] of the radiochemical yield is indicated by the data.

REFERENCES

1. D. Williams and P. Yuster, July 16th Nuclear Explosion: Total Radiation, Report LA-353, Los Alamos Scientific Laboratory, Aug. 27, 1945. (Classified).
2. J. A. Sanderson and H. S. Stewart, Measurements of Total Radiant Energy, Crossroads Test Technical Instrumentation Report. (Classified).
3. Scientific Director's Report of Atomic Weapons Tests, Operation Sandstone Measurements by NRL, Sandstone Report II, Annex 2, Part 1, Naval Research Laboratory Report 265. (Classified).
4. H. S. Stewart and J. A. Curcio, The Influence of Field of View on Measurements of Atmospheric Transmission, J. Opt. Soc. Am., 42: 801 (1952).
5. W. B. Fussell, Color Temperatures at Greenhouse, Tumbler-Snapper, Ivy, and Castle, NRL Report No. 4613, Series B, July 1955. (Classified).

Part III
Radiant Power as a Function of Time — Photoelectric Measurements

C. C. PETTY

Naval Research Laboratory
Washington, D. C.

January 1955

ABSTRACT

The brightness temperature of each of the Operation Greenhouse fireballs was measured in two wavelength regions as a function of time. The measurements were made with high-speed filtered photoelectric systems located at Parry Island. A time resolution of 10 to 15 μsec was obtained.

The spectral power incident on Parry Island, as a function of time, is also reported for two wavelength bands, one centered at 6200 A and the other at 3520 or 3720 A. These data are presented without atmospheric correction and are thought to be good to 25 per cent, except in the case of the George shot.

By using supplementary data on fireball area supplied by Edgerton, Germeshausen & Grier, Inc. (EG&G) and applying an atmospheric correction, equivalent black-body brightness temperatures of the fireballs, as a function of time, were obtained. In general, it can be said that an agreement exists in these temperatures between shots. First maximum temperatures varied from

PREFACE

This report covers one of two phases of work done under the project titled Radiant Power as a Function of Time. The report on the second phase dealing with bolometer equipment has appeared separately as Report NRL-4875.

ACKNOWLEDGMENT

Acknowledgment is made of the assistance rendered in this work by Hugh Raymond, James Perry, and Sidney Rattner, and the co-operation of EG&G.

1 OBJECTIVE

The objective of this measurement was to determine an equivalent black-body temperature of an atomic bomb explosion as a function of time. The original intent was to calculate the color temperature from continuously measured ratios of the spectral flux densities in two wavelength regions. This could not be accomplished with the data obtained at Operation Greenhouse. However, it was possible to determine brightness temperatures as a function of time, as well as to collect other information valuable as a part of a general store of information concerning atomic devices.

2 BACKGROUND

2.1 Development of Techniques

The technique used at Operation Greenhouse for the measurement of spectral energy as a function of time within two wavelength intervals utilized two photomultiplier systems—the response of one peaked at 3720 A for the first shot and at 3520 A for the last three shots; the response of the other peaked at 6200 A. The signals from the photomultipliers were recorded through the use of appropriate amplifiers, oscilloscopes, and cameras. The ratios of the spectral flux densities determined by these measurements were to be used to calculate color temperatures.

Measurements of this type were attempted at Operations Crossroads and Sandstone. At Operation Crossroads, the wrong sensitivity was selected, and no data were obtained. The theoretical aspects of this experiment and the method of data reduction are adequately described in the Operation Crossroads report.[1] At Operation Sandstone,[2] William Ogle made photoelectric measurements with a time resolution of 0.01 sec. He presented his results in terms of illumination measured in "suns," i.e., the number of times the illumination as produced by the noontime sun in that region.

At Operation Greenhouse, using the red and blue channel method indicated above, it was hoped that the first 100 μsec of the detonation could be covered with a resolution of 1.0 μsec and the first millisecond with a resolution of 10 μsec. A high-speed photomultiplier-oscillograph-camera system was used for measuring and recording rapid variations in the intensity of luminous flux.

2.2 Theory

The measurement of spectral irradiance in a narrow wavelength band as a function of time, in conjunction with a knowledge of the solid angle subtended by the explosion as a function of time, may be used to assign temperatures to the surface of an explosion, when it is assumed or demonstrated that the surface radiates as a black body. This is the so-called brightness temperature. The brightness temperature cannot be greater than the true temperature because the emissivity of a body cannot exceed unity at any wavelength.

When the solid angle subtended by the explosion is not known, a color temperature can be determined for the surface of an explosion if the spectral irradiance is measured in two wavelength bands. The color temperature of a source is the temperature of a black body which emits radiation that has the same spectral distribution as that from the source. The color temperature may be higher or lower than the true temperature, depending on the way in which the emissivity varies with wavelength. In the special case of a nonselective or gray body, the color and true temperatures are necessarily identical.

This determination of color temperature is valid provided the temperatures encountered do not enter the Rayleigh-Jeans region (i.e., where $\lambda\theta \gg C_2$). (To attain the same accuracy with the Rayleigh-Jeans law as with Planck's law—one per cent, $\lambda\theta$ must exceed 77 cm deg.) To illustrate, let the sensitivity of a photoelectric cell at wavelength λ be S_λ in microamperes

per watt. A filter with a transmission T_λ is placed over the photocell. For a sensitive area of b square centimeter, the photocurrent I in microamperes resulting from normal incident light is

$$I = b \int_{\lambda_1}^{\lambda_2} H_\lambda T_\lambda S_\lambda d\lambda, \tag{1}$$

where H_λ is the spectral irradiance of the incident light in watts per square centimeter per wavelength interval. The limits of integration, λ_1 and λ_2, are the system cutoffs, e.g., the filter cutoff ($T_{\lambda_{1,2}} = 0$), the photocell cutoff ($S_{\lambda_{1,2}} = 0$), etc.

If the incident light on the photocell comes from a Lambert or perfectly diffuse radiator, when the distance R from source to receiver is large compared to the dimensions of the radiator, the observed spectral irradiance, H_λ, is given by the equation

$$H_\lambda = \frac{J_\lambda t_\lambda}{R^2} \tag{2}$$

where t_λ is the atmospheric transmission between the source and receiver for wavelength λ and J_λ is the spectral radiant intensity of the surface at wavelength λ in units of watts.

From Planck's radiation law

$$J_\lambda = \frac{ac_1\lambda^{-5}}{\pi[\exp(c_2/\lambda\theta)-1]} \tag{3}$$

where c_1 and c_2 are radiation constants, a is the area of source in square centimeters, and θ is the temperature in degrees Kelvin.

Substituting values for H_λ and J_λ from Eqs. 2 and 3 into Eq. 1, we obtain

$$I = \frac{abc_1}{\pi R^2} \int_{\lambda_1}^{\lambda_2} \frac{\lambda^{-5}}{\exp(c_2/\lambda\theta)-1} t_\lambda T_\lambda S_\lambda d\lambda \tag{4}$$

In the Rayleigh-Jeans region, the expression for the photocurrent becomes simpler. In this region, $\lambda\theta \gg c_2$ and Eq. 4 take the form

$$I = \frac{abc_1\theta}{\pi R^2 c_2} \int_{\lambda_1}^{\lambda_2} \lambda^{-4} t_\lambda T_\lambda S_\lambda d\lambda \tag{5}$$

If a second photoelectric cell is used in a system with a different band pass and its current and constants are represented by primed symbols, the ratio of the two photocurrents will be

$$\frac{I'}{I} = \frac{b' \int_{\lambda_1'}^{\lambda_2'} \frac{\lambda^{-5}}{\exp(c_2/\lambda\theta)-1} t_\lambda T_\lambda' S_\lambda' d\lambda}{b \int_{\lambda_1}^{\lambda_2} \frac{\lambda^{-5}}{\exp(c_2/\lambda\theta)-1} t_\lambda T_\lambda S_\lambda d\lambda} \tag{6}$$

This expression cannot be solved explicitly for θ. However, a curve can be drawn by assuming values of θ and calculating the ratio of I'/I. Then the experimental I'/I ratio can be compared to the curve to obtain an estimate of the black-body color temperature.

In the Rayleigh-Jeans region, Eq. 6 becomes

$$\frac{I'}{I} = \frac{b' \int_{\lambda_1'}^{\lambda_2'} \lambda^{-4} t_\lambda T_\lambda' S_\lambda' d\lambda}{b \int_{\lambda_1}^{\lambda_2} \lambda^{-4} t_\lambda T_\lambda S_\lambda d\lambda} \tag{7}$$

or I'/I is the constant, since the temperature of the source no longer appears in the expression. Hence the measurement of spectral irradiance in two wavelength bands in this region

would not yield a unique color temperature for an explosion. In fact, the experimental value of I'/I must be different from the value of I'/I in Eq. 7 by more than the experimental error in order that this be a valid method of determining a black-body temperature.

It was hoped in this work to calculate color temperatures, but it so happened that the range of temperatures experienced, coupled with the large experimental error due to the measurements having to be taken over such a long path and thus introducing enormous atmospheric correction, brought the data within the above indeterminate category. Therefore it was necessary to return to Eq. 4 and calculate the brightness temperature. In order to do this, supplementary data on fireball area was necessary. This was supplied from the camera studies of EG&G. Since a characteristic brightness temperature could be calculated for two wavelength bands, the validity of the assumption of a black-body distribution could be ascertained, at least for the interval between the two bands of wavelengths involved.

3 INSTRUMENTATION

3.1 General Description

A high-speed photomultiplier-oscillograph-camera system was constructed to measure and record rapid variations in the intensity of luminous flux. The bandwidth of the system was such that the waveforms of the luminous flux variations were exactly reproduced if Fourier components of less than 200 kc/sec were present and reproduced with minor distortions if Fourier components of less than 425 kc/sec were present.

One data channel consisted of a 1P21 photomultiplier tube optically filtered for a narrow band of wavelengths in the red portion of the visible spectrum, a preamplifier, a delay line, three oscilloscopes set at different gain levels, recording cameras, and associated power supplies and timing-mark generators. The second data channel was identical except that an ultraviolet narrow-band filter replaced the red filter. A third photomultiplier circuit triggered the oscilloscope sweeps for both data channels.

The photomultiplier tube used had an S-4 spectral response with peak sensitivity at 4000 A. The over-all system had a dynamic range of 2000 to 1 (66 db) and the minimum recordable flux was 0.2×10^{-9} watt/cm^2. The red channel was filtered for a narrow band of wavelengths centered on 6200 A and the ultraviolet channel on 3720 A for the first shot and 3520 A for the other shots. The change from 3720 to 3520 A was made because very strong absorption occurs near 3720 A in most atomic explosions. Figures 1 and 2 show the relative response of both channels for all tests.

The selection of these channels was guided by the desire to have them as far apart spectrally as possible but still within a region for which the atmospheric attenuation was moderate and known. Unfortunately, as indicated previously, both because of the temperatures encountered and the distances at which the equipment was operated, the choice did not prove satisfactory.

The signal from each photomultiplier was presented to three oscilloscopes in parallel. Each scope amplifier was adjusted to a different gain in order to cover a large dynamic signal range. The oscilloscope traces were photographed on 35-mm film by means of General Radio cameras for 1.4 sec with increased time resolution during the first 100 μsec. Timing marks were produced every 10 μsec by Z blanking and every 1000 μsec by a light flash.

In addition to the two data channels, the system incorporated a trigger channel. Delay lines were placed in the data channels but not in the trigger channel so that the oscillograph X-sweep started 2 to 3 μsec before the data signals arrived at the Y deflection plates.

The equipment, although designed for use within 5 km of the bomb, was set up on Parry Island. Thus the distance involved between shots and station ranged from 16 to 35 km, much beyond the efficient range of the equipment as noted. A complete description of the original equipment is included in the appendix of this report.

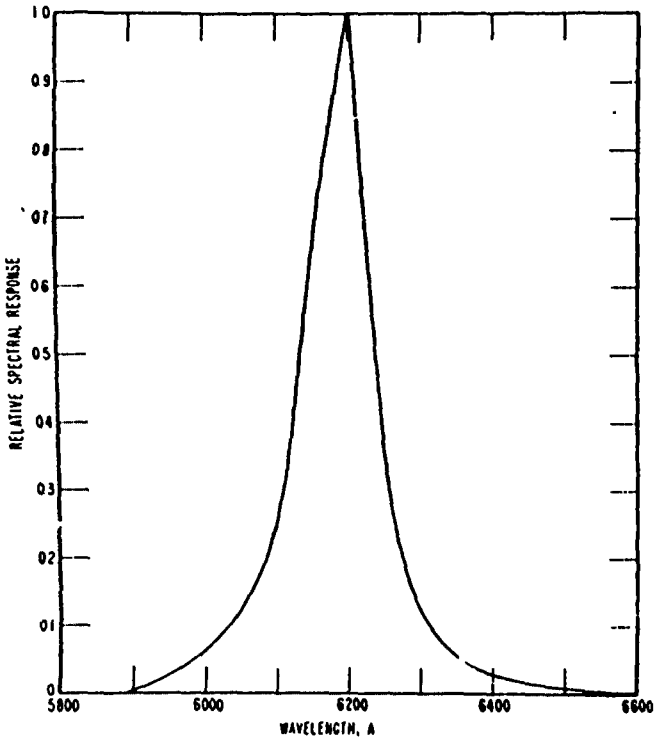

Fig. 1 — Relative spectral response of red channel.

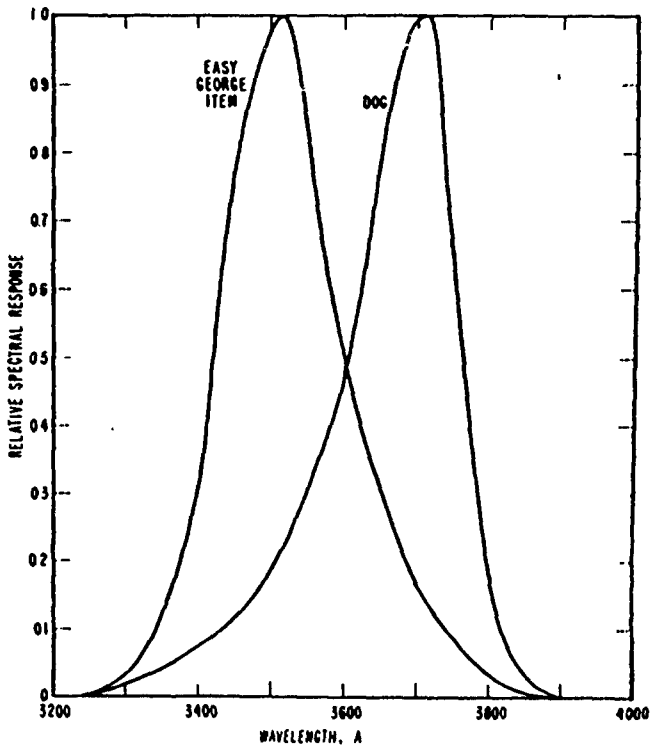

Fig. 2 — Relative spectral re ponse of blue channel.

3.2 Calibrations

The calibration of the photoheads was accomplished by use of a 1000-watt lamp with a known candlepower and relative spectral intensity. A radiation level convenient to simple field setup was used. The 1000-watt lamp was mounted 1 ft in front of the photoheads, with a square-wave light chopper giving rise to pulses of 1000 cps. The response level of the photosystems was adjusted both by use of the oscilloscope gain controls and by variation in the size of the apertures directly in front of the phototubes. The calibration levels so obtained were always less than the anticipated flux levels to be encountered during the shots, hence the over-all sensitivity of the system was adjusted for the shots by the addition of Wratten neutral density filters mounted in front of the apertures of the phototubes.

The deviation from neutrality of the filters in the ultraviolet was measured, and appropriate corrections were made in the analysis of the data. Atmospheric and field-of-view corrections were also made from measurements taken 1 hr before each shot.

3.3 Field Modification of Equipment

The equipment was operated as described above for the Dog shot. However, a few days before the Easy shot, failure of components in the photomultiplier power supplies necessitated changes in the equipment as follows: Two Model 306 d-c power supplies, made by the Atomic Instrument Company, were used to power the photomultipliers in the data channels, while a battery pack powered the trigger photohead. The change in power supplies required a redesign of the photoheads and introduction of bleeder resistors across the dynodes. The delay lines used with this setup consisted of 50 ft of RC-65/U cable, giving a delay of approximately 2 μsec. These modifications were used for the remaining three shots.

Consideration of the data from the Dog shot indicated that the low-frequency response of the 250 A oscilloscope, when operated as an a-c scope, was not adequate for proper reproduction of the flux vs. time curve beyond the minimum. Therefore, for the remaining three shots, one scope in each data channel was operated as a d-c scope while the two others were operated as a-c scopes for higher sensitivity.

3.4 Performance of Equipment

The special sweep circuit that was built into the 250 A oscilloscope for the purpose of increasing the time resolution during the first 70 μsec of the explosion functioned properly only for the Item test. The cathode-ray tube was rotated so that the X-axis sweep took place in the vertical direction. During the driven sweep, the spot moved vertically downward from the top of the screen with an exponentially decreasing velocity, remaining at the bottom of the screen for 4 to 5 sec. The oscilloscope screens were photographed by General Radio type 651-AG 35-mm strip cameras, started at about 0.5 sec before the explosion. In most cases the starting of the cameras triggered the oscilloscopes so that the added time resolution of the special sweeps was lost. In these cases the time resolution was limited by the film travel rate of the General Radio cameras and was 10 to 15 μsec.

Weather conditions just prior to the George shot introduced many difficulties in connection with the photocell equipment. The shelter in which the equipment was housed was not rainproof, and many times following showers there were several inches of water in the shelter. These conditions may have been responsible for the fact that, as determined by the acceleration of the cameras, the power line fuse in the shelter blew at about 30 msec before zero time on the George shot, cutting off the power to the oscilloscopes and cameras. Nevertheless, traces were recorded of the first maximum on several cameras, and these data are presented in this report. It is thought that the ratio of deflections recorded for the red and ultraviolet channels corresponds roughly to the ratio of incident power in the two wavelength regions, even though the absolute calibration of each channel is probably not good.

4 RESULTS

4.1 General

The original intent of the photocell measurements—viz., the determination of fireball color temperatures from the ratio of flux measured in the red and ultraviolet spectral regions—could not be accomplished from the data. However, many useful data were obtained in the form of curves giving, as a function of time, the incident power or spectral irradiance at Parry Island in watts per square centimeter per micron for both spectral regions.

Data were obtained for all shots, and the curves are presented with no corrections, atmospheric or otherwise (see Figs. 3 to 6). The values are thought to be good to 25 per cent, except in the case of George shot where the power line fuse blew just prior to zero time. This caused a greater uncertainty in the George data. The curves were obtained by using a combination of traces obtained from each of the three sensitivity ranges employed for each data channel because it was impossible for one scope to be on scale during the first maximum and also during the minimum.

4.2 Dog Shot

Both channels were on scale in the first maximum. A second maximum appeared only in the red channel and was followed by a large negative deflection. In the ultraviolet channel, the oscilloscope trace showing the greatest deflection faded out at 90 msec and the spot did not reappear until about 1 sec later. After the minimum, the next most sensitive scope in the ultraviolet channel showed a large negative deflection comparable to that in the red channel. There was no apparent reason for these large negative deflections, and nothing comparable was recorded for later shots. Figure 3 shows the oscilloscope deflections for the Dog shot as a function of time, the ordinates being converted to incident power at Parry Island.

4.3 Easy Shot

The scaling on this shot was not good. Both channels were considerably off scale in the first and second maxima and the only usable data were obtained in the neighborhood of the minimum. Figure 4 shows the usable oscilloscope deflections for this shot, reduced to incident power, at Parry Island.

4.4 George Shot

Traces were obtained on both channels for the first maximum even though the power line fuse blew at about 30 msec before zero time. The ultraviolet channel was on scale; the trace for the red channel was off scale by an estimated factor of 2 because of failure of the least sensitive scope in that channel. Gain ratios in each channel persisted in spite of the blown fuse; it is believed that the deflection ratio between the red and ultraviolet channels is in approximate correspondence to the incident power ratio for the two wavelength regions. Figure 5 is a plot of the George shot deflections, as a function of time and reduced to incident power, at Parry Island.

4.5 Item Shot

This is the only shot for which the special sweeps functioned properly, giving increased time resolution in the first 20 μsec. The ultraviolet channel was on scale at the first maximum, but the red channel was off scale on all scopes, yielding data only during the first 100 μsec and in the neighborhood of the minimum on the d-c scope. The data for the first 100 μsec show clearly that the initial light from the bomb is at the red end of the spectrum, whereas the

Pages 50-51
Deleted

ultraviolet light appears 50 μsec or so later. Teller light triggered the oscilloscopes and appeared in the ultraviolet channel, but it was not reproduced accurately because neither the delay line nor the oscilloscopes had high-frequency characteristics sufficient to follow such a sharp pulse. Figure 3.4 is a plot of the oscilloscope deflections for the Item shot, reduced to incident power, at Parry Island.

5 ANALYSIS OF DATA

5.1 Color Temperature

The original intent of these photoelectric measurements could not be accomplished with the data obtained. Basically, the reason for this was that for the temperatures experienced the two wavelengths measured fell on a part of the distribution curve showing constant slope so that unique temperatures could not be determined from the ratio method.

Furthermore, the photocell equipment had originally been designed to be used at stations close to the shot towers, i.e., at sites M, P, and N, and for such distances a wide field of view was appropriate. The equipment, because of operational logistics, was actually used at Parry Island. From this distance the error due to light scattered into the field of view of an instrument would be serious unless proper corrections were made. The atmospheric corrections necessary were not accurate enough for the assignment of temperature values from the power ratios. For example, a factor of 3 in the ratio could mean a difference in black-body color temperature of [illegible] whereas corrections for light scattered into the field of view of the photomultiplier units ran as high as a factor of 10.

5.2 Corrections

5.2.1 Atmospheric

The transmission of the atmosphere, as a function of wavelength, was measured at approximately 1 hr before each shot over a horizontal path running from Parry Island to Eniwetok Island.

For the Dog and the Easy shots, the transmission of the atmosphere at approximately 5500 A was measured between the cab of the shot tower and one of the ground stations—site M for Dog shot and Parry Island for Easy. For the George and Item shots, the slant transmission for visible light was computed from total thermal data taken at two distances from the explosion.

A marked gradation in scattering as a function of altitude had been observed in the area, and it was anticipated that the horizontal and slant measurements would not agree. This was found to be the case, and in computing the slant spectral transmission, the measured transmission from the shot tower to the ground station was considered to represent the slant transmission at 5500 A. Furthermore, the slant spectral transmission was believed to be different from the horizontal transmission only because of a lower average density of neutral scattering particles in the path. Therefore, the spectral transmission values obtained from the horizontal measurements were multiplied by a constant factor to make the transmission at 5500 A coincide with the values predicted from the measurement between the tower and the ground station.

The effect of scattering, as a function of the field of view of the measuring equipment and of the atmospheric transmission, has been measured by Curcio and Stewart.[3] These measurements were checked at Eniwetok during Operation Greenhouse where greater path lengths and lower transmission values than those in the above report were encountered. Thermocouples with fields of view ranging from 3 to 25 degrees in diameter viewed the explosions from Parry Island to see if the approximate equation for the effect of scattered light described in reference 1 holds under these conditions. The average results of these thermocouple investigations show that the equation calls for a scattered light correction about 25 per cent too great for the

wide fields of view at Parry Island. Therefore, in computing the scattered light correction for the photomultipliers, the theoretical correction factor was multiplied by 0.8.

Table 1 shows the computed values of the slant spectral transmission to Parry Island, used in the reduction of the photocell data. It also lists the fields of view of the photoelectric equipment and the computed ratio of scattered to unscattered flux received in the red and ultraviolet wavelength regions.

Table 1 CORRECTIONS USED IN ANALYSIS OF PHOTOCELL DATA

Shot	Wavelength, A	Slant transmission to Parry Island from shot	Diameter of field of view, degree	Ratio of scattered to unscattered flux	Spectral distribution correction factor	Inverse square correction factor, 10^{13} cm^2
Dog	6200	0.18	50	0.9	1.03	3.34
	3720	0.11	50	1.7	1.01	
Easy	6200	0.090	34	1.6	1.02	13.4
	3520	0.022	34	7.6	0.95	
George	6200	0.063	34	2.4	1.02	7.67
	3520	0.025	29	6.0	1.30	
Item	6200	0.070	34	2.2	1.02	13.4
	3520	0.014	34	12.6	1.05	

5.2.2 Spectral Distribution

The calibration source used in these measurements had a spectral intensity distribution equivalent to that of a black body at a temperature of 2690°K. Such a distribution falls off rapidly in the ultraviolet and is peaked at about 11,000 A. However, the distribution of the bomb, at least at the time of its peak emission, was more nearly that of Rayleigh-Jeans, which falls off toward the red according to the inverse fourth power of wavelength. A source-emitting radiation with a Rayleigh-Jeans distribution and positioned so that it produced unit irradiation at the photomultiplier for the wavelength of peak response of the photomultiplier-filter combination did not produce the same signal as the calibration source positioned to produce unit irradiation for the same wavelength. This was because of the finite band pass of the interference filters. The use of the non-neutral Wratten filters and the atmosphere further complicated the situation. However, correction for these effects was made by dividing the Rayleigh-Jeans distribution into the product of the photomultiplier sensitivity curve and the transmission of the optical components present during the shot and comparing the integrated effect of this combination to that of the calibration source distribution divided into the same product. Spectral distribution correction factors were calculated in the above manner for all four Operation Greenhouse tests and are listed in Table 1. These factors were computed by dividing the Rayleigh-Jeans sensitivities by those for the calibration source; in all cases except that of the ultraviolet channel used for the George shot, the corrections were 5 per cent or less. The smallness of these corrections was due to the fact that the atmospheric and Wratten-filter transmission tended to change the spectral distribution of the bomb to a distribution more nearly that of the calibration source. In the case of the ultraviolet channel at the George shot, a density 2.5 filter was introduced which had an extremely sharp cutoff in the ultraviolet, requiring a 30 per cent spectral distribution correction.

5.3 Brightness Temperature

Brightness temperatures can be roughly approximated by making the atmospheric correction to the spectral power and then taking into account the inverse-square law and the area of

the fireball as given by Eq. 4. The black-body temperatures so obtained represent temperatures of a black body emitting the same spectral power per unit area of surface as that calculated for the bomb.

These temperature calculations for the four shots were derived from values of the fireball area obtained from EG&G. These areas are given in Fig. 7. They are subtended areas and must be multiplied by four to convert to total surface area. Brightness temperatures were calculated by use of these areas and a knowledge of the distance between the receivers and the bomb.

5.3.1 Dog Shot

Figure 8 shows the results obtained for this shot. The spectral power radiated from a unit surface area of the fireball, as a function of time, is shown. The scale on the right side of a figure indicates the temperature of a black body which would radiate the spectral power per unit area given on the scale at the left. A first maximum temperature of at 0.2 msec is indicated for the red channel and at 0.2 msec for the blue channel. The red channel registered a second maximum temperature of at 200 msec; no data were obtained on the second maximum temperatures on the blue channel.

5.3.2 Easy Shot

The results of this shot are shown in Fig. 9. No first or second maximum temperatures are indicated because of improper scaling of the equipment.

5.3.3 George Shot

The temperature variations for this shot are shown in Fig. 10. A first maximum temperature of at 0.2 msec is indicated for the red channel and at 0.3 msec for the blue channel. No second maximum temperatures are indicated.

5.3.4 Item Shot

The results of this shot are shown in Figs. 11 and 12. A first maximum temperature of at 0.1 msec is indicated for the 6200 A region and at 0.3 msec for the 3520 A channel. The second maximum temperature on the blue channel was at 250 msec. There were no data in the red channel at the second maximum. Figure 12 shows the power per unit area at 6200 A, radiated during the early stage of the Item shot. Since no information was available on the area of the Item shot during the interval from zero to 100 μsec, the early Easy area data were used in these computations. The curve was then normalized so that at 100 μsec the value of brightness temperature determined in this manner coincided with the value represented in Fig. 11. A curve of this sort was not drawn for the 3520 A channel because it is believed that the small rise in the neighborhood of 1 to 30 μsec is due to Teller light and such an intensity measurement cannot be interpreted in terms of surface brightness through the use of fireball areas.

6 CONCLUSIONS

When these results are interpreted in terms of the spectral power radiated from a unit area of the fireball, their accuracy is limited by the accuracy of the atmospheric corrections. The most serious correction is that for the radiation scattered into the field of view of the measuring equipment by the atmosphere, and it is most serious for low values of atmospheric

Pages 55-57 Deleted

transmission. The computed ratio of scattered to unscattered flux for the photoelectric equipment varied from 0.9 to 12.6 for the four shots, but, despite such large corrections, the equivalent black-body temperatures are in rough correspondence between shots. Figure 13 summarizes the data of Figs. 8 to 12, in terms of temperature as a function of time. The computed temperatures at the first maximum varied from about [redacted] and at the second maximum the temperatures computed for the two cases for which data were obtained—viz., Dog at 6200 A and Item at 3520 A—were both around

Fig. 13—Summary of fireball temperatures.

Contrary to predictions, all the data obtained indicate an increase in surface brightness from the onset of the explosion. This reached a peak and then declined following the theoretical curve before increasing again to a second maximum. The only data obtained with the increased time resolution, viz., that for the Item shot, indicated an increasing surface brightness at 6200 A in the 10 to 100 μsec interval when the areas for Easy shot were applied. Also, the brightness temperature computed from the Item area at 100 μsec for both wavelength regions was around [redacted] The Item data show clearly that the light from the bomb is predominantly at the red end of the spectrum during the first one-hundred microseconds.

Appendix 1: General Description of High-Speed Photomultiplier Equipment

The complete high-speed photomultiplier system consisted of the following sections:

1. Photoheads and associated power supply.
2. Red data channel equipment rack.
3. Blue data channel equipment rack.
4. Auxiliary electronic equipment rack.
5. Camera switch boxes.

and had the following performance characteristics:

1. Field of view, 30° diameter.
2. Spectral response: yellow, 0.61 to 0.63 μ; blue, 0.36 to 0.38 μ.
3. Noise level <1.0 mv referred to photohead output.
4. Minimum detectable signal, 2×10^{-9} watt/cm^2.
5. Rise time, 1.2 μsec.
6. Dynamic range, 2000.
7. Duration of recording, 1.4 sec.
8. Film speed; 100 ft/sec max; 70 ft/sec av.

Luminous flux falling on the photohead passed through a light filter which limited to a narrow band of wavelengths the flux which actually fell on the photocathode of the multiplier tube. The photomultiplier tube converted the variations in luminous flux to a varying electrical signal (with instantaneous amplitude proportional to the density of the incident flux) which passed through the output cathode follower stage in the photohead to a coaxial cable connecting the photohead to the data channel equipment rack.

At the data channel rack, the data signal entered the "Y-amp Input" terminals of three oscillographs connected in parallel. These oscillographs were Dumont type 250-A which had been modified in the following manner: The cathode-ray tube was rotated on its axis so that the X-axis sweep took place in a vertical direction. The sweep circuit was modified so that during the first 70 μsec after the "driven sweep" was triggered the spot moved vertically downward from the top (top center with no Y signal) of the screen with an exponential relationship between displacement and time, and remained at the bottom (bottom center with no Y signal) of the screen for the duration of the sweep, which was 4 or 5 sec. The data signal (Y signal) applied to the oscillograph during the triggered sweep time deflected the spot from the center line.

Triggering of both data channels was caused by a signal from a third photohead, which had no light filter. A delay line was placed in the data channels but not in the trigger channel so the sweep would be initiated 2 to 3 μsec before the data signals arrived at the deflecting plates of the cathode-ray tubes.

The horizontal deflection of the spot on the oscillograph screen was photographically recorded by a General Radio type 651-AG 35-mm strip camera. The motion of the film was in the opposite direction to the vertical motion (of the spot image), which took place during the first 70 μsec of sweep, thus producing increased time resolution during this period. The film drive was started approximately 0.5 sec before the sweep was triggered and was nearly up to maximum by the time the data signal arrived.

It was found necessary to increase the brightness of the oscillograph spot by increasing the cathode-ray tube accelerating potential from 3400 to 4700 volts. This was done because of the high film speed required to obtain the desired time resolution. In addition to this increase of accelerating potential, an auxiliary intensifier circuit that decreased the grid-cathode potential acted during the first 100 μsec (i.e., moving part of the sweep) only.

The three oscillographs on each data channel rack (Y-Inputs connected in parallel) were set so that the "Y-Gains" were in the ratio 1:1, 10:1, and 100:1, respectively. This procedure had the effect of increasing the dynamic range of data measurement. The maximum dynamic range (ratio of maximum to minimum readable signal) of a single oscillograph with a 5-in. screen was 50, but because of the circular screen and camera focusing problems, this range was reduced to approximately 20. The use of three oscillographs with gain ratio of 10 increased the dynamic range by a factor of 100; hence the over-all dynamic range was 2000.

Two sets of timing marks appeared on the film. A 100 kc/sec pulse generator connected to the Z-Input of each oscillograph blanked out the cathode-ray tube beam for a fraction of a microsecond every 10 μsec. This produced 10 μsec timing marks. A timing light and holder was attached beside the screen of each oscillograph and a small mirror deflected a spot of light which flashed at 1000 cps into the lens of the camera. The timing light was driven by a

1000-cps pulse shaper which was in turn driven by a 1000-cps American Time Products frequency standard. This produced 1000 μsec timing marks on the side of the film.

Figure 14 shows the functional block diagram of one data channel equipment and its associated units. One complete data channel consisted of the following sub units:

1. Data channel photohead.
2. Trigger channel photohead.
3. Photohead power supply.
4. Three Dumont 250-A oscillographs (modified).
5. Three General Radio 651-AG 35-mm cameras.
6. Three timing lights and holders.
7. Three 1000-cps pulse shapers.
8. American Time Products 1000-cps frequency standard.
9. Power distribution panel.
10. Triple unit 3-kv high-voltage supply.
11. 100 kc/sec marker pulse generator.
12. Remote-controlled camera switch box.

The other channel was identical in function and agreement to the above but one trigger channel photohead, one photohead power supply, and one 100 kc/sec marker pulse generator supplied both channels.

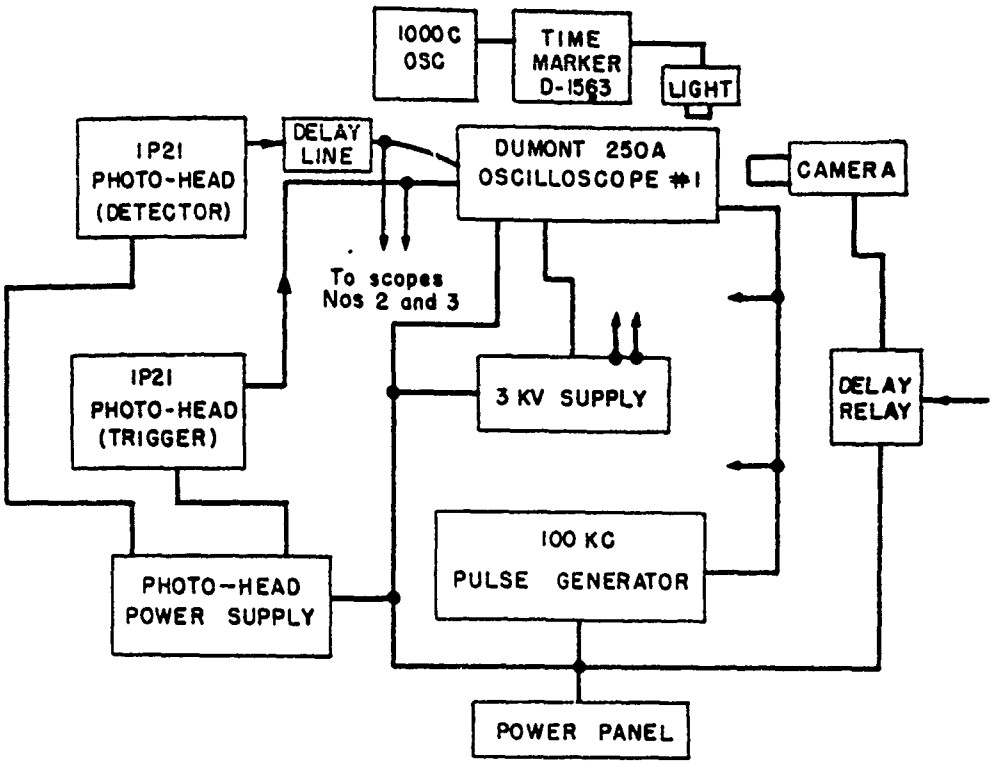

Fig. 14 — Block diagram of photomultiplier equipment.

REFERENCES

1. H. S. Stewart, Measurement of the Spectral Radiance of the Explosion at 3600 A and 9400 A as a Function of Time, Crossroads Project VI-2 Report, XR-311, Mar. 14, 1947.
2. W. Ogle, Sandstone Report No. 14, July 28, 1948.
3. J. A. Curcio and H. S. Stewart, The Influence of Field of View on Measurements of Atmospheric Transmission, J. Opt. Soc. Am., 42:801(1952).

Appendix A
Identification of the Teller Light Emission Spectrum

LOUIS F. DRUMMETER, JR.

Radiometry II Branch, Optics Division
Naval Research Laboratory
Washington, D. C.

February 18, 1954

ABSTRACT

The short-duration emission spectrum (Teller Light), which occurs in the air around a nuclear weapon at the time of the nuclear reaction, was photographed with low spectral resolution at Operation Greenhouse in 1951. Twenty-six emission lines were recorded. Twenty-three of these have been definitely ascribed to the second positive band series of the neutral nitrogen molecule. The remaining three are identified as the 0–0, 0–1, and 0–2 bands of the first negative series of the singly ionized nitrogen molecule. These bands occur in the region 3100 to 4700 A. Structure above 5500 A exists but cannot be ascribed definitely to the Teller flash and cannot be analyzed well because of the low dispersion of the spectrum in this region.

PREFACE

This report covers a portion of the information obtained under the Naval Research Laboratory Program (NRL-H) Thermal Radiation Project at Operation Greenhouse. It concerns a phenomenon (Teller Light) that is of particular interest to a large number of people who are perhaps not at all concerned with other optical manifestations of a nuclear explosion. For this reason, this information is assembled as an individual report.

Program NRL-H was under the direction of Dr. Wayne Hall. The Thermal Radiation Project was under the direction of Dr. Harold Stewart of the Optics Division. Dr. Stewart invented the cine spectrographs used in obtaining the records described in this report. The spectrographs were operated in the field by D. J. Lovell and B. Engel of NRL.

1 OBJECTIVE

The release of visible and ultraviolet radiation by an exploding nuclear weapon occurs in three stages: Teller Light, first maximum, and second maximum. The NRL-H Thermal Radiation Project included the specific objectives of recording the spectra of these stages with the aim of establishing (1) the spectral distribution of the energy radiated in each stage and (2) the

identity of the atoms or molecules which might give rise to the spectral structure of the radiation.

It was felt that the spectral distribution of the radiation would yield the color temperature of the fireball. The structure of the spectrum should yield information concerning the mechanism of the radiating process.

2 INTRODUCTION AND BACKGROUND

2.1 Nature of Teller Light

Teller Light is the short-duration flash of light that appears in the air surrounding a nuclear weapon at the time the nuclear reaction takes place. The flash is caused by excitation of the air, first by gamma radiation and then by neutrons; it exists for some hundreds of meters around the weapon. The flash is named after Edward Teller, who explained it on the basis of intense gamma excitation.

The emission of the flash at Trinity was observed by Geiger, Mack, and Nicholson,[1] who recorded, spectrographically, eleven emission lines but were unable to identify the lines. The existence of a distinct neutron flash was first discovered by the NRL group under Dr. Stewart in the spring of 1952.

2.2 Greenhouse

At Operation Greenhouse, in 1951, further spectroscopic studies of nuclear weapons were undertaken by the Optics Division of NRL. One type of observing instrument used was the high-speed or cine spectrograph[2] developed at NRL. This is a low-dispersion low-resolution prism type instrument which records spectra at the rate of 5000 per sec. During the course of Operation Greenhouse, the cine spectrographs produced a number of excellent spectra of Teller Light, and these spectra were studied during 1951 and early 1952 in an attempt to identify the emission spectrum. The results of this study are given in the following sections. Actually, the conclusions drawn here were presented informally in early 1952 to the Los Alamos staff, but this is the first formal presentation of the results.

3 INSTRUMENTATION AND RECORDING

3.1 The Cine Spectrographs

The cine spectrographs used at Operation Greenhouse and described in reference 2 are moving-image moving-film devices which produce spectra on 70-mm film at the rate of 5000 per sec. Each spectrum is exposed for approximately 180 μsec. Each exposure actually produces four adjacent spectra, which are displaced laterally with respect to each other but which differ from each other only in intensity. Figure 1 shows the appearance of a single 180-μsec exposure. The four adjacent spectra are numbered in intensity sequence and an arrow indicates the direction of displacement. The least intense spectrum is almost too faint to see.

3.2 Teller Light Records

Because the Teller flash was shorter than 180 μsec, the spectrograph did not always produce a clean Teller spectrum. If the flash was recorded early in the exposure cycle, then early bomb light obliterated the flash spectrum. Despite this effect, a number of excellent Teller Light spectra were obtained. Figure 1 shows a positive print of one of the spectra obtained. It will be noted that the spectrum consists mainly of discrete emission bands or broad lines. In Figure 1, the wavelengths are noted for a number of lines in the most intense, number one, spectrum. The broad structure in the red end of the spectrum is not necessarily part of the Teller spectrum and will be discussed later.

4 MEASUREMENTS AND RESULTS

4.1 Preliminary

Twenty-six discernible lines on two of the best spectra were measured on a comparator and checked against a wavelength curve derived by making comparator measurements on a

Fig. 1—Cine-spectrogram of teller light. (Arrow indicates displacement of spectra 1, 2, 3, and 4. Indicated wavelengths refer to lines in No. 1 spectrum.)

mercury-arc spectrum obtained with the same spectrograph. The wavelength measurements were rather poor because the standard mercury spectrum was not adjacent to the Teller spectrum. However, the wavelengths were adequate to indicate that except for three lines there was excellent correlation with the second positive bands of the neutral nitrogen molecule. Accordingly, twenty-three of the emission lines were tentatively identified with the second positive band series of nitrogen as listed in reference 3.

4.2 Detailed Analysis

Three of the Teller lines were then assigned the corresponding N_2 wavelengths listed in reference 3, and the wavelengths of the other lines were calculated relative to these three lines. Table 1 gives the results obtained by establishing a Hartmann formula based on the three assumed wavelengths. It will be seen that 23 out of 26 lines correspond with the published wavelengths of the heads of the N_2 bands within less than 4 A. The other three lines agree nicely with the wavelengths of bands of the first negative series of the singly ionized nitrogen molecule.[3]

Table 2 lists the observed transitions for N_2, together with the estimated intensities of the Teller lines and the corresponding intensities listed in reference 3. There is excellent agreement on relative intensities, and the observed transitions are those one would expect to find in nitrogen.

5 CONCLUSIONS

The evidence is convincing that most of the Teller lines observed at Operation Greenhouse are, in reality, emission bands corresponding to the second positive series of neutral nitrogen. The remaining lines are assignable to the first negative band series of the singly ionized nitrogen molecule. The N_2^+ transitions observed are the prominent 0–0, 0–1, and 0–2, in agreement with what one would expect.

The structure in the red end of the spectrum cannot be clearly assigned to Teller Light. It may equally well be very early bomb light superimposed in the flash spectrum. It was expected that the mechanism that excited the second positive series of nitrogen would also excite the first positive series which constitutes a complex structure at wavelengths above 5000 A. The low dispersion of the spectrograph in this region makes it impossible to tell from the Operation Greenhouse spectra whether this series is present or whether the exposure in this region is purely bomb light.

TABLE 1—COMPARISON OF MEASURED WAVELENGTHS WITH BAND-HEAD LISTINGS FOR N_2 AND N_2^+

It appears that no structure is visible below 3000 A where the 2–0, 3–0, and 3–1 transitions of N_2 would be expected. This may be because the radiation in this region is attenuated by the normal atmosphere or because the lines were not emitted strongly. It may also be that O_3 was formed around the bomb by gammas and attenuated these wavelengths. O_3 would also account for the anomalous weak intensity of the 1–1 transition at 3339 A where O_3 has an absorption band.

TABLE 2—COMPARISON OF ESTIMATED INTENSITY WITH INTENSITIES LISTED IN THE LITERATURE FOR THE SECOND POSITIVE NITROGEN BANDS

Transitions	Estimated Teller intensity	Pearse and Gaydon intensity for N_2
0–0	10	10
0–1	10	10
0–2	10	10
0–3	8	8
0–4	6	4
0–5	2	0
1–0	6	9
1–1	1	2
1–2	6	8
1–3	8	10
1–4	8	9
1–5	6	5
1–6	4	2
2–1	6	8
2–2	2	2
2–3	4	4
2–4	6	8
2–5	6	8
2–6	4	6
2–7	2	3
3–2	4	6
3–4	1	0
3–8	4	3

REFERENCES

1. Geiger, Mack, and Nicholson, Preliminary Report on the Spectrum and Radiation of the July 16, 1945, Nuclear Explosion, Report LA-588, Los Alamos Scientific Laboratory, Sept. 16, 1947.
2. D. J. Lovell, H. S. Stewart, and S. Rosin, The Cine Spectrograph, NRL Progress Report, pp. 19, June 1953.
3. R. W. B. Pearse and A. G. Gaydon, The Identification of Molecular Spectra, 2nd. ed. rev., pp. 168 and 176, John Wiley & Sons, Inc., New York, 1950.

Appendix B
Atlas of High-Dispersion Spectra

J. A. CURCIO

Radiometry II Branch, Optics Division
Naval Research Laboratory
Washington, D. C.

September 1, 1954

ABSTRACT

This appendix is an atlas of microphotometer traces made from high-dispersion spectrograms obtained in the spring of 1951 for the Dog, Easy, George, and Item shots at Operation Greenhouse. The various spectral structures are identified on the traces, and the wavelengths of prominent lines are noted at intervals of several angstrom units.

Among the prominent spectral features in molecular absorption are the Schumann-Runge bands of O_2. Atmospheric absorption due to O_2 and H_2O (water vapor) is also very pronounced. Present also are the absorption spectra of Fe, Na, Ba, Mn, and other minor constituents.

PREFACE

A successful attempt was made to obtain high-dispersion spectra at each of the four shots in the Operation Greenhouse series. The results are presented in this report in the form of microphotometer traces.

The spectra considered here were the first high-dispersion records ever obtained from nuclear explosions. Some identifications, however, were not made until after spectra were available from the Buster–Jangle series. Some of the latter spectra provided simplified keys for the identification of much mysterious structure in the Operation Greenhouse plates, e.g., the Schumann-Runge bands of O_2.

The work was part of the NRL-H Thermal Program and was under the direction of Dr. H. S. Stewart and the general supervision of Dr. W. C. Hall.

The production of this atlas would have been impossible without the advice, assistance, and technical skills of William Pringle, Allen Petusen, and others in the Naval Research Laboratory Graphic Arts Group, headed by Warren Ramey.

1 INTRODUCTION

This appendix presents an atlas of microphotometer traces of four high-dispersion spectrograms made during Operation Greenhouse in the spring of 1951. These spectra were recorded with a Baird two-meter grating spectrograph. Spectra were made on 4- × 10-in. plates in the first order and covered a range of 2000 A per plate at a dispersion of about 8.1 A/mm.

The range was varied from shot to shot. The traces were made with a Leeds & Northrup recording microphotometer using a plate scanning speed of 1 mm/min and a chart speed of about 2 in./min. The denser spectra were measured at higher sensitivity. A sensitivity change is noted on the traces as a scale change.

Each recorded spectrum consists of several steps of varying intensity, since a step wedge was placed in the stigmatic position of the spectrograph when the spectra were made. The traces reproduced in this atlas are composites compiled from the steps of different densities in the same spectrum. Specific portions of the traces were selected to make a single composite for a particular shot solely to illustrate structural detail and to maintain wavelength continuity.

As shown here, the traces are simply plots of optical density on the plate vs. wavelength. The density grid which is normally present on the paper has been eliminated for the sake of clarity in reproduction. The original continuous microphotometer traces are reproduced in 100 A sections, two sections to a page, at about a three-fold reduction. Each section overlaps slightly the preceding and subsequent sections.

The Dog, Easy, and Item plates were measured on a Mann Comparator and all wavelengths and identifications were transferred to the traces. Identification of structures in the spectrum from the George shot was made by comparing the trace with that from the Dog trace. The Dog spectrum showed a structure similar to that of the George spectrum and had been thoroughly measured. The identification of spectral structure was aided by frequent references to the publications.

1.1 Shot Dog

The Dog spectrum was recorded on a II-O plate for the total time-of-light output and covers the wavelength region 3000 to 5000 A. The original trace is a composite of several steps as is evident in the reproductions. The absorption structure is predominantly Fe and O_2 (Schumann-Runge). The Schumann-Runge system has been detailed on the trace and the various bands have been indicated. A noteworthy feature of this spectrum is the complete absence of Fe below about 4000 A. This is in contrast to the later Buster-Baker spectrum in which the Fe occurs equally strong throughout the same 3000 to 5000 A wavelength interval. Presence of Ba, Sr, Ti, Mn, Zn, and OH is also indicated. There is indication of weak NO_2 absorption on the original plate but it is not apparent on the trace.

1.2 Shot Easy

The shot Easy spectrum was recorded on a II-F plate for the total time-of-light output and covers the wavelength range of 5000 to 7000 A. The original trace is a composite of two steps as is evident in the reproduction. This spectrum shows only absorption structure due mainly to atmospheric O_2, atmospheric H_2O (water vapor), Fe, and Ba. Minor structure of other elements is also indicated. The most striking feature of this plate is the very strong water vapor absorption. It is probable that some of the unidentified structure may be some hitherto unobserved water vapor lines.

1.3 Shot Item

The shot Item spectrum was recorded on a II-N plate for total time-of-light output and covers the wavelength range of 7000 to 9000 A. The original trace is a scan of the most intense step on the plate. This spectrum shows very strong absorption structure due to atmospheric O_2 and H_2O (water vapor). The atomic oxygen structure at 7770 is strongly evident. Minor structure of other elements is also indicated. It is probable that some of the unidentified lines may be due to water vapor.

1.4 Shot George

The shot George spectrum was recorded on a II-O plate for the total time-of-light output and covers the wavelength range of 3000 to 5000 A. The original trace is a composite of three steps as is evident in the reproduction. The absorption structure is predominantly Fe and O_2 (Schumann-Runge). This spectrum is very similar to that of shot Dog and shows the characteristic absence of Fe below about 4000 A. The Schumann-Runge system has been detailed on the trace, and the various bands have been indicated. Presence of Ba, Sr, Ti, Mn, Zn, and Cr is also indicated.

REFERENCES

1. Harold D. Babcock and Charlotte E. Moore, The Solar Spectrum, λ6600 to λ13495, Carnegie Institution of Washington, Publication 579, 1947.
2. George R. Harrison, M.I.T. Wavelength Tables, John Wiley & Sons, Inc., New York, 1939.
3. W. Lochte-Holtgrenen and G. H. Dieke, "Uber die ultravioletten Banden usw," Ann. Phys. Lpz. 3: 937 (1939).
4. M. Minnaert, G. F. W. Mulders, and J. Houtgast, A Photometric Atlas of the Solar Spectrum, D. Schnable, Kampert and Helm, Amsterdam, 1940.
5. Orren C. Mohler, A. Keith Pierce, Robert R. McMath, and Leo Goldberg, Photometric Atlas of the Near Infrared Solar Spectrum, University of Michigan Press, Ann Arbor, Michigan, 1950.
6. R. W. B. Pearse and A. G. Gaydon, The Identification of Molecular Spectra, 2nd ed. rev., John Wiley & Sons, Inc., New York, 1950.
7. C. E. St. John, C. E. Moore, L. W. Ware, E. F. Adams, and H. D. Babcock, Revision of Rowland's Preliminary Table of Solar Spectrum Wavelengths, Carnegie Institution of Washington, Publication 396, 1928.

2. MICROPHOTOMETER TRACES

2.1 Shot Dog*

Date: 4-8-51
Type shot: Tower
Yield,
Temperature, °C: 26.11
Relative humidity, %: 74.1
Water P, mm: 18.80
Distance, m: 16,200
Wavelength coverage: 3000 to 5000 A
Exposure: Total time

*Data taken from Report LA-1329, The Spectroscopy of Nuclear Explosions, by G. H. Dieke. This report also contains the mass of various materials involved in the construction of the weapon.

Pages 70-79
Deleted

2.2 Shot Easy*

Date: 4-21-51
Type shot: Tower
Yield, kt: 46.7
Temperature, °C: 26.66
Relative humidity, %: 71.4
Water P, mm: 19.08
Distance, m: 32,300
Wavelength coverage: 5000 to 7000 A
Exposure: Total time

*Data taken from Report LA-1329, The Spectroscopy of Nuclear Explosions, by G. H. Dieke. This report also contains the mass of various materials involved in the construction of the weapon.

GREENHOUSE - EASY
GREENHOUSE - EASY

GREENHOUSE - EASY
GREENHOUSE - EASY

GREENHOUSE - EASY
GREENHOUSE - EASY

GREENHOUSE - EASY
ORIGIN & BAND (3,2,0)
GREENHOUSE - EASY

GREENHOUSE - EASY
B - fo
A - H_2O
GREENHOUSE - EASY
B - fo
A - H_2O
SCALE CHANGE
ORIGIN
BAND (1,4,0)

GREENHOUSE - EASY
■ - Fe
▲ - H2O
ORIGIN ▲ BAND (1, 3, 2)
GREENHOUSE - EASY
■ - Fe

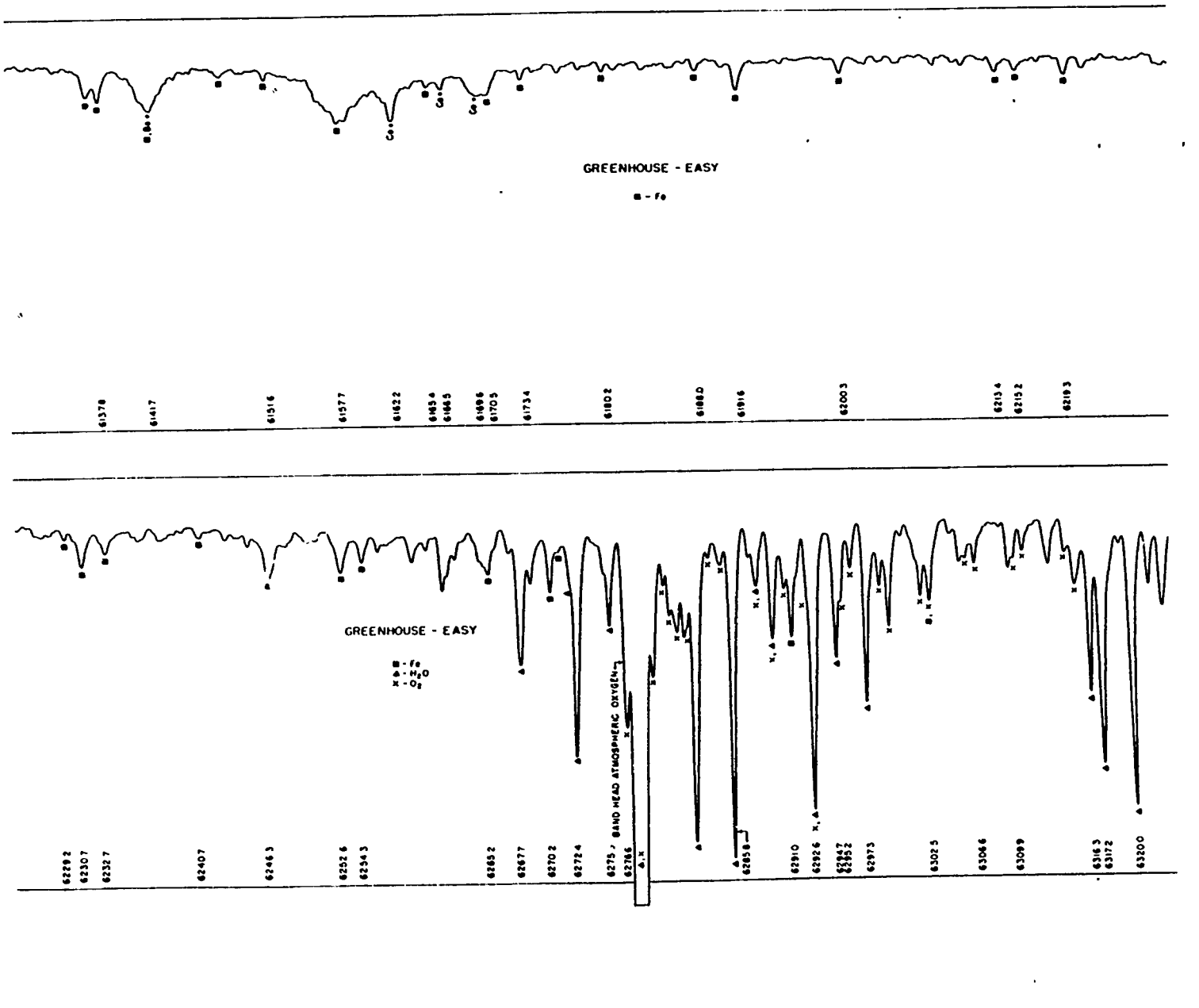
GREENHOUSE - EASY
■ - Fe
GREENHOUSE - EASY
X - H_2O
O_2
62292
62307
62327
62407
62463
62526
62543
62652
62677
62702
62724
62752
62785
62858
62910
62926
62942
62952
62973
63025
63046
63099
63163
63172
63200

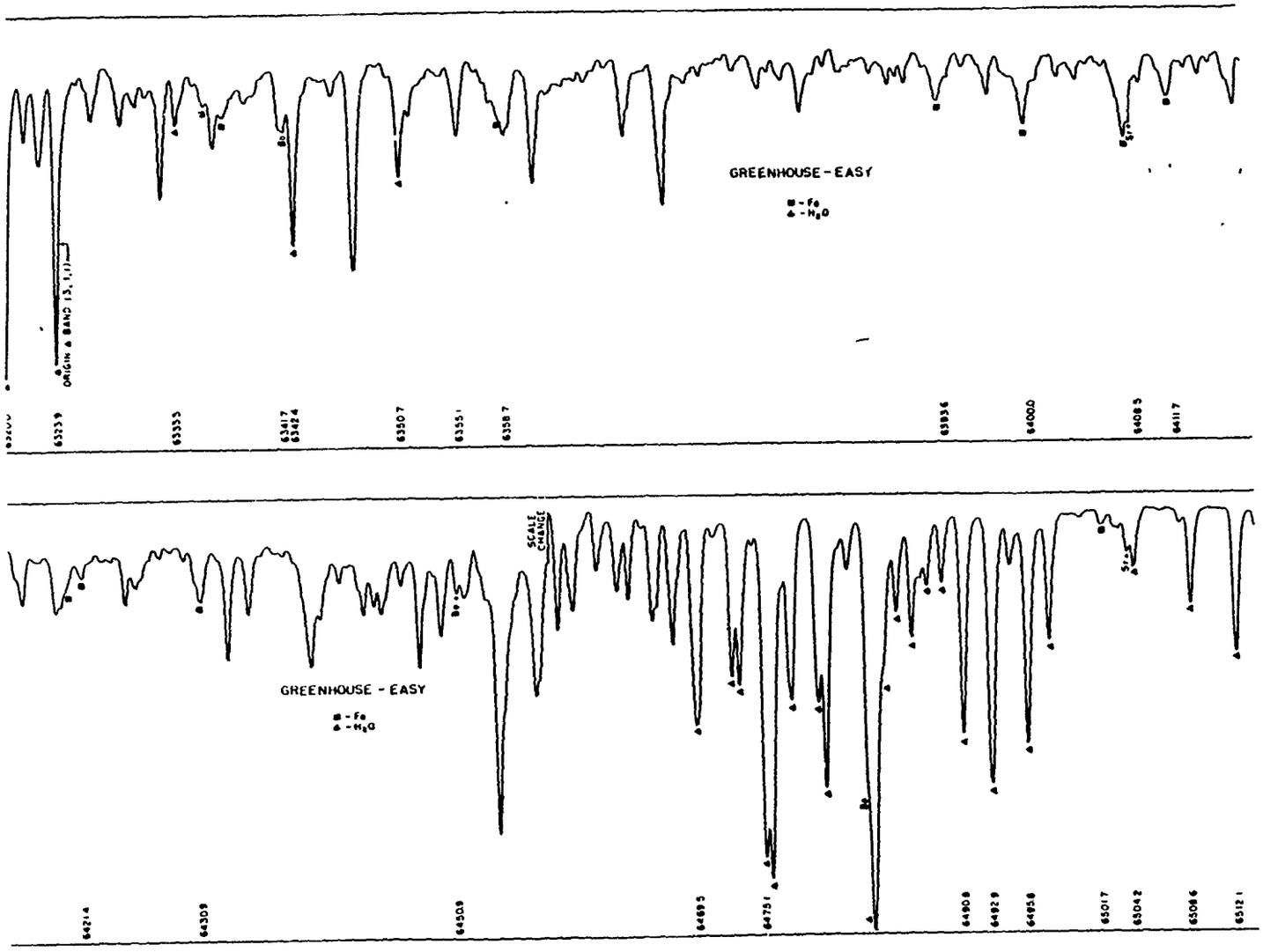
GREENHOUSE - EASY
■ - Fe
▲ - H_2O
ORIGIN & BAND (3, 1, 1)
63239
63333
63417
63424
63507
63551
63587
63836
64000
64085
64117
SCALE CHANGE
GREENHOUSE - EASY
■ - Fe
▲ - H_2O
64214
64309
64509
64693
64751
64908
64929
64958
65017
65042
65086
65121

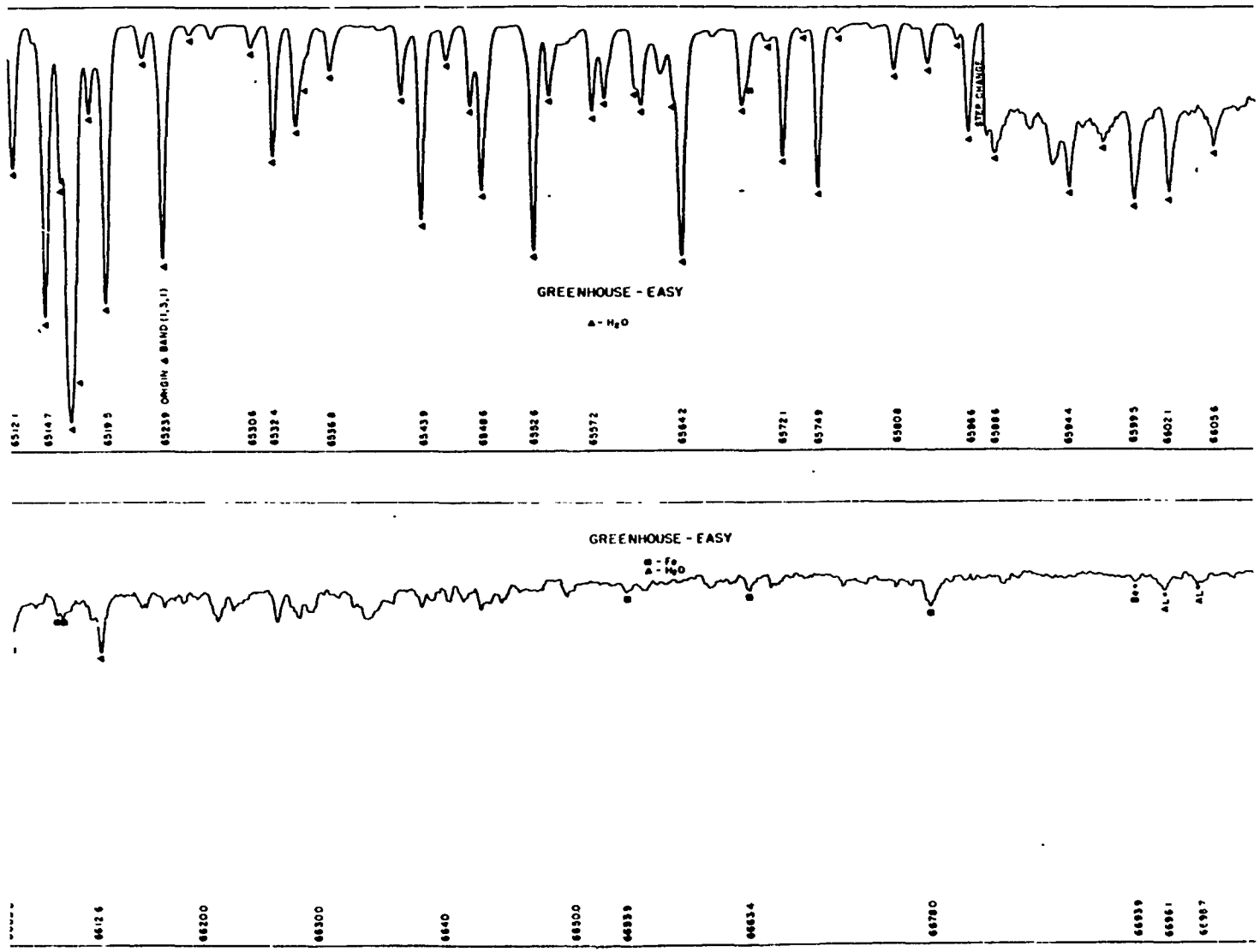
GREENHOUSE - EASY
▲ - H_2O
STEP CHANGE
GREENHOUSE - EASY
■ - Fe
▲ - H_2O

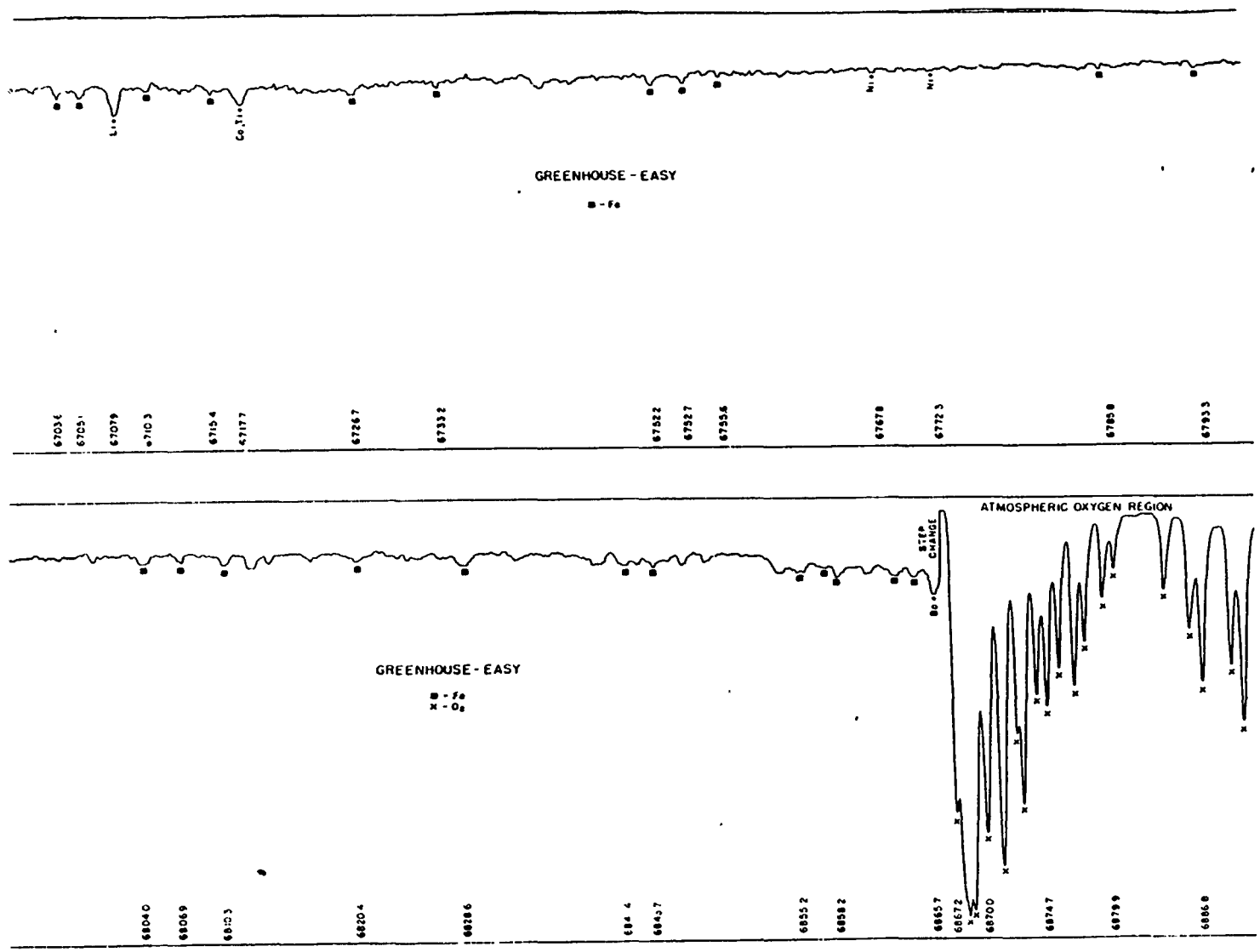
GREENHOUSE - EASY
■ - Fe
ATMOSPHERIC OXYGEN REGION
STEP CHANGE
GREENHOUSE - EASY
■ - Fe
× - O2

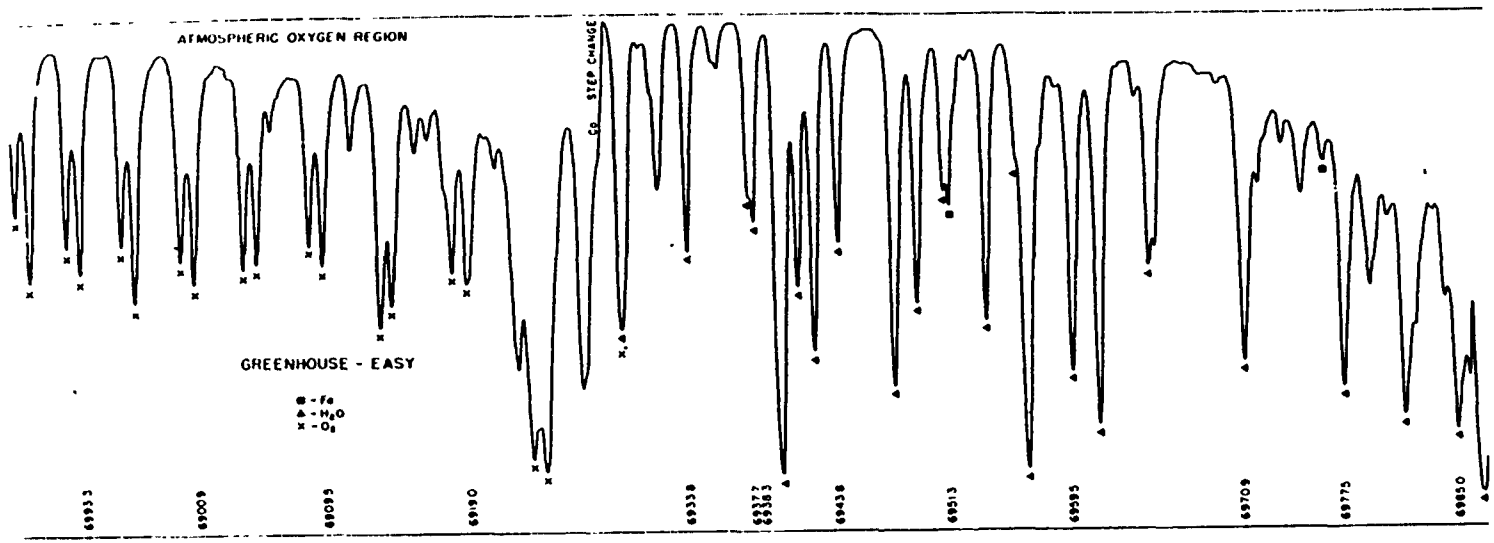
ATMOSPHERIC OXYGEN REGION
GO STEP CHANGE
GREENHOUSE - EASY
● - Fe
▲ - H_2O
× - O_2
69353
69009
69095
69190
69338
69377
69383
69438
69513
69585
69709
69775
69850

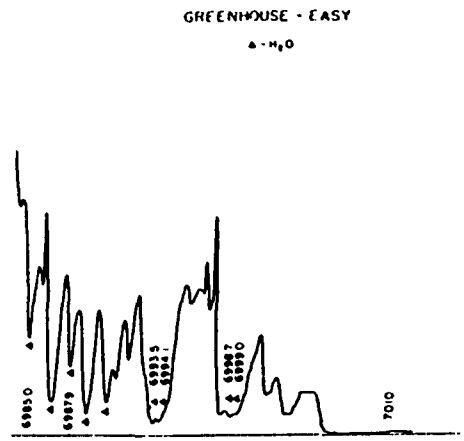
GREENHOUSE - EASY
▲ - H_2O
69850
69879
69915
69923
69967
69990
7010

2.3 Shot Item*

Date: 5-25-51
Type shot: Tower
Yield,
Temperature, °C: 26.83
Relative humidity, %: 78.3
Water P, mm: 20.73
Distance, m: 32,300
Wavelength coverage: 7000 to 9000 A
Exposure: Total time

*Data taken from Report LA-1329, The Spectroscopy of Nuclear Explosions, by G. H. Dieke. This report also contains the mass of various materials involved in the construction of the weapon.

Pages 93-103 Deleted

2.4 Shot George*

Date: 5-9-51
Type shot: Tower
Yield:
Temperature, °C: 27.22
Relative humidity, %: 87.5
Water P, mm: 23.70
Distance, m: 24,800
Wavelength coverage: 3000 to 5000 A
Exposure: Total time

*Data taken from Report LA-1329, The Spectroscopy of Nuclear Explosions, by G. H. Dieke. This report also contains the mass of various materials involved in the construction of the weapon.

Pages 105-114
Deleted